

Propagation of light in Plasmonic multilayers

Rabih Ajib

▶ **To cite this version:**

Rabih Ajib. Propagation of light in Plasmonic multilayers. Electromagnetism. Université Clermont Auvergne [2017-2020], 2017. English. NNT : 2017CLFAC040 . tel-01789097

HAL Id: tel-01789097
https://theses.hal.science/tel-01789097

Submitted on 9 May 2018

HAL is a multi-disciplinary open access archive for the deposit and dissemination of scientific research documents, whether they are published or not. The documents may come from teaching and research institutions in France or abroad, or from public or private research centers.

L'archive ouverte pluridisciplinaire **HAL**, est destinée au dépôt et à la diffusion de documents scientifiques de niveau recherche, publiés ou non, émanant des établissements d'enseignement et de recherche français ou étrangers, des laboratoires publics ou privés.

N° d'Ordre : D.U. 2812

UNIVERSITE CLERMONT AUVERGNE

ECOLE DOCTORALE DES SCIENCES FONDAMENTALES
N° 911

THESE

présentée pour obtenir le grade de

DOCTEUR D'UNIVERSITE

Spécialité: Physique

Par **«AJIB Rabih»**

Master en Sciences de la Matiére

Propagation of Light in Plasmonic Multilayers

Soutenue publiquement le « *12 Mai 2017* », devant la commission d'examen.

Président et rapporteur : TALIERCIO Thierry
Rapporteure : LITMAN Amélie
Directeur de thèse : MOREAU Antoine
Coencadrant: AJALTOUNI Ziad

Acknowledgements

I want to take this opportunity to thank all who helped me during the years I spent working on this project. First of all, I would like to express my special appreciation to my advisors Professor Antoine Moreau and Professor Ziad Ajaltouni. You have been tremendous mentors for me. I would like to thank you for encouraging my research and for allowing me to grow as a research scientist. Your advices on both research as well as on my career have been priceless. A special and a great thanks is for my supervisor Prof. Antoine Moreau for all the time you gave me, for all the support you have given me. You have always been there for me when I needed you. Thank you sincerely. I have learned a lot from you Antoine.

I would also like to thank the members of my committee ; Prof. Amélie Litman and Prof. Thierry Taliercio for serving as my jury members. Thank you for accepting to examine my PhD manuscript in addition to judging my whole work.

A special thanks is for my teachers in the Master 2 that I held at Université Clermont Auvergne. I have really benefited from all the knowledge I acquired from all of you.

In addition, I would like to thank my colleagues at group ELENA and LHCB. All of you have been there to support me when I recruited patients and collected data for my Ph.D. thesis.

I would also like to thank all of my friends from all nationalities who supported me throughout my years of research, and incensed me to strive towards my goal. I would like also to take this opportunity to be grateful to a precious friend.

A sincere thanks to the person that was more like a big brother to me. Thanks to my big brother Dr. Fadi Zoubian. Thank you for being on my side a great and honorable person that I can never pay you back.

A special thanks to my great family back in Lebanon. Words cannot express how grateful I am to my father, my mother, my brother in law, my big sister and her kids, and my young sisters and my brother for all of the sacrifices that you've made on my behalf. Your prayers for me and your presence in my life was what sustained me thus far.

Finally, I have the honor to dedicate all the work and success done in this PhD thesis to my Idol and to the person that I have always looked up high to. This PhD thesis is dedicated to you Baba, it is for you ABO LJOOJ!

Contents

Acknowledgements iii

Introduction 1

1 Solving Maxwell's equations in multilayers 5
1.1 Maxwell's equations and constitutive relations 5
1.1.1 General expression for the fields 6
1.1.2 Boundary conditions 8
1.1.3 Scattering matrix algorithm 9
Interface scattering matrix 9
Layer matrix 9
Cascading of scattering matrices 9
1.1.4 Scattering matrix of the whole structure 10
1.1.5 Examples 10
Refraction 11
Brewster incidence 11
Total internal reflection 12
Anti-reflective coating 12
Bragg mirror 12
Negative refraction 13
Perfect lensing 13
1.2 Guided modes 18
1.3 Different light velocities 19
1.3.1 Phase and group velocities 19
1.3.2 Energy velocity 20
1.4 Conclusion 22

2 Plasmonics 23
2.1 Drude's model 23
2.2 Surface plasmons 26
2.2.1 Dispersion relation of the surface plasmon 27
2.2.2 Group velocity 30
2.2.3 Energy velocity 31
2.2.4 Dispersive case 33
2.3 Prism couplers 34
2.3.1 SPR bio-sensors 36
2.4 Metallo-dielectrics 38
2.5 Gap-plasmons 40
2.5.1 Dispersion relation 43
2.5.2 Group velocity 44

2.5.3 Energy velocity 45
2.5.4 Prism coupler and gap-plasmons 46
2.6 Conclusion 47

3 The Energy Point of View in Plasmonics: The Concept of Plasmonics Drag 51
3.1 Energy velocity in metals 51
3.2 Energy flow for surface plasmons 54
3.2.1 Energy velocity 54
3.2.2 Poynting flux 56
3.3 Energy balance for gap-plasmons 56
3.3.1 Poynting flux 57
3.3.2 Integrated energy density 58
3.3.3 Energy velocity 60
3.4 Conclusion 61

4 Beyond Drude's Model: Non-locality in Plasmonics 63
4.1 Local and nonlocal polarizability 64
4.1.1 Polarizability in Drude's model 64
4.1.2 Polarizability in the hydrodynamic model framework . 65
4.2 Non-Locality 67
4.3 Gap-Plasmon Resonance and non-locality 69
4.4 Conclusion 72

Conclusion 73

Bibliography 75

List of Figures

1 Nano-particle Resonance in Stained Glass . . . 2
2 Lycurgus cup . . . 2

1.1 Refraction . . . 11
1.2 TM . . . 12
1.3 Brewster Incidence . . . 13
1.4 Total internal reflection . . . 14
1.5 Anti Reflective Coating . . . 14
1.6 Transmission . . . 15
1.7 Bragg . . . 15
1.8 Bragg . . . 16
1.9 Negative refraction . . . 16
1.10 Perfect Lens . . . 17
1.11 Guided Modes . . . 20

2.1 Skin Depth . . . 27
2.2 Surface plasmon . . . 28
2.3 The Surface Plasmon dispersion relation . . . 29
2.4 Otto Configuration . . . 36
2.5 Otto . . . 37
2.6 The critical angle . . . 37
2.7 Reflection coefficient as a function of the critical angle . . . 38
2.8 Kretschmann Configuration . . . 39
2.9 Kretschmann Raether Configuration . . . 40
2.10 Biosensing apparatus . . . 40
2.11 Kretschmann-Raether Configuration for biosensing . . . 41
2.12 Figure taken from [37] illustrating the dispersion properties of hyperbolic meta materials in the wave vector space. . . . 42
2.13 Negative refraction . . . 42
2.14 MIM Waveguide . . . 44
2.15 The effective index . . . 47
2.16 Gap Plasmon Resonance . . . 48
2.17 Gap Plasmon . . . 49

3.1 Poynting ratio . . . 57
3.2 Poynting ratio . . . 60

4.1 Gap-plasmon prism coupler . . . 69
4.2 Local/Non-local . . . 70
4.3 Local/Non-local . . . 71

To my family…

Introduction

Nanophotonics is the field of science aiming at manipulating light using nano-sized structures, allowing for an unprecedented control over some of the most exotic light-matter phenomena. These nanostructures can be made of dielectrics, transparent materials. In that case, their size is usually of the order of the wavelength and they are called photonic crystals. Another way to control light is to leverage the very peculiar response of tiny pieces of metal, or of nano-structures metallic films to reach very high field concentrations. A piece of metal can actually be considered as plasma (the free electron gas) trapped in a box (the piece itself). That is the reason why the domain of nanophotonics dealing with metals is called plasmonics.

While Maxwell's equations were published 150 years ago[26, 27], when used with Drude's model established more than 100 years ago[15] they are perfectly able to describe accurately the optical response even of the smallest nanoparticles. We know it because starting maybe 30 years ago, Maxwell's equations began to be solved computationally using first specifically designed numerical methods. This is the case of the Fourier Modal Method[17, 22], which is widely used in nanophotonics and has been partly developed in the team Elena of the Institut Pascal to which I belong.

However, the systematic resolution of Maxwell's dates back to Abeles[1] who proposed a transfer matrix formalism for multilayers that has had a tremendous success in the optical community. The team recently published a set of numerical tools for the optics of multilayers called Moosh[12]. I participated in this effort, helping to test the programs extensively. Multilayers clearly belong to the class of nanostructures, like anti-reflective coatings that are usually only a quarter of wavelength thick, or the periodic multilayers called Bragg mirrors and that are composed equivalently of thin layers. The optical properties of multilayers, despite having been largely studied, are still nowadays a very active domain of research. This is mainly due to the fact that including metallic layers vastly expands the potential effect of multilayers on light - allowing negative refraction and sub-wavelength focusing.

Multilayered plasmonic structures are crucial, as studying their optical properties help understand the resonances of nanoparticles, coupled or not to a metallic film. An interface between a metal and a dielectric actually supports a surface plasmon - and this in turn explains why a spherical nanoparticle can resonate: the surface plasmon sees the particle as a cavity. They resonate whenever the circumference is a multiple of the surface plasmon effective wavelength. A gap between two metals supports a gap-plasmon, which explains why a nano cube coupled to a metallic surface resonate: it constitutes a cavity for the gap-plasmon, and the resonance condition is here that the cube should have a width that is a multiple of half an

effective wavelength of the gap-plasmon[29].

This is just to show how fundamental the study of multilayered structures is - essentially because it allows analytic results and provides a physical insight into all the other structures of plasmonics. We underline here that plasmonics is much older than most people suspect, as the absorption properties of metallic nanoparticles have been empirically found and used in stained glass (see Fig. 1) and even in precious objects made of glass during the roman era (see Fig. 2). Nowadays, nanoparticles are considered serious candidates for the thermal treatment of cancer - owing to their unique light concentration properties.

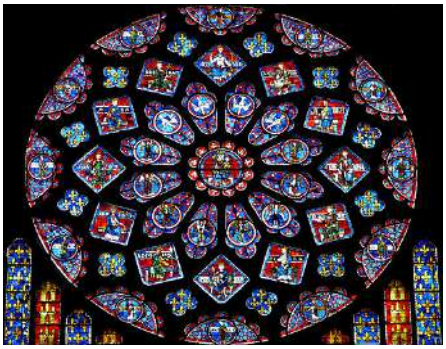


FIGURE 1: Nano-particle plasmonic resonances are utilized in stained glass to produce colorful pictures.



FIGURE 2: Lycurgus cup is the oldest example of a glass containing nanoparticles for an optical purpose.

Plasmonic guided modes present a unique and very specific property: they can present very low effective wavelengths. This explains why the size of plasmonic resonators can be reduced to a deeply subwavelength size. Even this aspect is well described using the classical description of guided modes, a more physical and simple explanation would be welcome. The main goal of my thesis was initially to give a more physical reason why plasmonic guided modes behave as they do, presenting very high effective index, by considering them with the point of view of energy propagation. Finally, despite its extraordinary accuracy, it seems that Drude's model actually presents some limitations[11] and that this is linked directly to the

small effective wavelength of plasmonic guided modes[28]. Since Moosh is able to take these phenomena into account, they have attracted my attention too.

In a first chapter, I will go through the way Maxwell's equations are solved in multilayers whether to find a reflection coefficient or a guided mode and its properties. I will explain the scattering matrix method that constitutes the core of Moosh. Throughout the whole manuscript I have tried to illustrate the concepts of nanophotonics and especially plasmonics using Moosh (Multilayer Optics is Officially Super Hype[12]).

In a second chapter, I will focus on plasmonic guided modes and metallo-dielectric multilayers, using again Moosh as a tool to explore all these situations. I will explain the first steps that led us to the generalization of Yariv and Yeh's theorem stating that the energy velocity, for mode guided in non-dispersive multilayered dielectric structures, is equal to the group velocity. We knew we would run into problems when trying to generalize this theorem to plasmonic guided modes because the energy balance should obviously include the contribution of free electrons - they are responsible for the optical response of metals and are moved by the electric field, the carrying a part of the energy of the wave. We have tried to see how easy the theorem could be generalized by calculating the group and energy velocity for the most emblematic guided modes (the surface plasmon and the gap-plasmon). This indicated us that after all, the free electrons could be forgotten in the energy balance.

In the third chapter, I will show that Yariv and Yeh's approach can be generalized to plasmonic structures, and that this provides a new insight into the fundamental reasons why plasmonic guided modes have such high effective indexes. We introduce the concept of *plasmonic drag* to summarize the insight the theorem brings and show on the examples of surface plasmons and gap-plasmons the energy balance that can be made.

Finally, in a fourth chapter, I have made a short study of a gap-plasmon resonance that is sensitive to the spatial dispersion present in metals. It is induced by the repulsion between free electrons, which is completely overlooked in Drude's model, but not in a more accurate description of the jellium: the hydrodynamic model. In this framework, exciting a gap-plasmon using a prism coupler is a good idea to put spatial dispersion into evidence.

Chapter 1

Solving Maxwell's equations in multilayers

In this first chapter, the way Maxwell's equations are solved in multilayers is presented. This is the principle of operation of Moosh[12], a program, developed by the team, which I have helped to test. I will show in this chapter the capabilities of Moosh, using it to illustrate the most fundamental concepts of optics - total internal reflection, positive or negative refraction and perfect lensing. I will then present the way Moosh finds the guided modes of a multilayered structure, as guided mode play a fundamental role in plasmonics.

1.1 Maxwell's equations and constitutive relations

In the 19^{th} century James Clerk Maxwell published the equations that govern electric and magnetic fields [27]. It was until that time that light have been considered to be an electromagnetic wave.

These equations depend on space and time and are given a follows

$$div\vec{D} = \rho \tag{1.1}$$

$$r\vec{o}t\vec{E} = -\partial_t\vec{B} \tag{1.2}$$

$$div\vec{B} = 0 \tag{1.3}$$

$$r\vec{o}t\vec{H} = \vec{j} + \partial_t\vec{D} \tag{1.4}$$

These equations are not complete without specifying the constitutive relations that are acceptable for isotropic, linear and local media. The equations are

$$\vec{B} = \mu_0 R_m * \vec{H} \tag{1.5}$$

$$\vec{D} = \varepsilon_0 R_e * \vec{E} \tag{1.6}$$

where $R_m(\vec{r},t)$ and $R_e(\vec{r},t)$ are the local responses of the medium. Where * is the convolution product with respect to time. A Fourier Transform with

respect to t can be done because the whole system is invariant with time. Then the constitutive relations become

$$\vec{B} = \mu_0 \mu(\vec{r}, \omega)\vec{H} \tag{1.7}$$

$$\vec{D} = \varepsilon_0 \varepsilon(\vec{r}, \omega)\vec{E} \tag{1.8}$$

The relative permitivity ε and the relative permeability μ depend on variables of space. In what follows we consider ε and μ to be constant. In addition, consider that the medium to be homogeneous(no source) for which ρ=0 and $\vec{j}$=0.

1.1.1 General expression for the fields

We consider lamellar structures of which ε and μ depend on z. In the harmonic regime, with a $e^{-i\omega t}$ time dependency, Maxwell's equations become

$$\partial_y E_z - \partial_z E_y = i\omega\mu_0\mu H_x \tag{1.9}$$

$$\partial_z E_x - \partial_x E_z = i\omega\mu_0\mu H_y \tag{1.10}$$

$$\partial_x E_y - \partial_y E_x = i\omega\mu_0\mu H_z \tag{1.11}$$

$$\partial_y H_z - \partial_z H_y = -i\omega\varepsilon_0\varepsilon E_x \tag{1.12}$$

$$\partial_z H_x - \partial_x H_z = -i\omega\varepsilon_0\varepsilon E_y \tag{1.13}$$

$$\partial_x H_y - \partial_y H_x = -i\omega\varepsilon_0\varepsilon E_z \tag{1.14}$$

Since the problem is invariant for x and y, a Fourier transform can be done with respect to these two variables. It is equivalent to say that we assume an $\exp i(k_x\, x + k_y\, y)$ dependency with respect to these two variables. Then, it is always possible to make a coordinate change in order to guarantee that $k_y = 0$, without loosing any generality. The important consequence is that there is no dependency on y any more and that Maxwell's equations decouple to split into two sub-systems, one where E_y plays a central role

$$\begin{cases} -\partial_z E_y = i\omega\,\mu_0\,\mu\,H_x \\ \partial_z H_x - \partial_x H_z = -i\omega\,\varepsilon_0\,\epsilon\,E_y\ , \\ \partial_x E_y = i\omega\,\mu_0\,\mu\,H_z \end{cases} \tag{1.15}$$

and one for which H_y (p polarization) is the central quantity

$$\begin{cases} -\partial_z H_y = -i\omega\,\varepsilon_0\,\varepsilon\,E_x \\ \partial_z E_x - \partial_x E_z = i\omega\,\mu_0\,\mu\,H_y \\ \partial_x H_y = -i\omega\,\varepsilon_0\,\varepsilon\,E_z \end{cases} \tag{1.16}$$

In plasmonics, the only interesting phenomena occur in p polarization[25].

Before continuing in the explanation of this section, it is essential to define what polarization of light is. Light, by definition, is an electromagnetic wave which consists of two wave forms, a vertical and a horizontal one in a certain direction of propagation. Up on polarization, only one component of the wave oscillates in a single direction. This means that if we choose a vertical polarizer, the horizontal component will be absorbed and vice versa. There are two types of polarization; P polarization where the transverse-magnetic (TM) is polarized it is thus called, tangential plane polarized. S- polarization, is also called transverse-electric (TE), as well as sigma-polarized or sagittal plane polarized.

The guided modes that are supported by metallo-dielectric structures, including a simple interface between a metal and a dielectric, are all based on oscillations of the electron gas that are linked to a magnetic field along the y direction here. If these guided modes are not excited, essentially nothing happens.

Combining the above equation in the p polarization case yields:

$$\partial_z \left[\frac{\partial_z H_y}{i\omega\mu_0\mu}\right] - \partial_x \left[\frac{\partial_x H_y}{i\omega\mu_0\mu}\right] = -i\omega\varepsilon_0\epsilon H_y \tag{1.17}$$

and finally

$$\partial_z^2 H_y + \partial_x^2 H_y = -\omega^2\varepsilon_0\mu_0\varepsilon\mu H_y \tag{1.18}$$

which is simply Helmholtz's equation for H_y. In s polarization, the result is exactly the same, except that H_y is replaced by E_y.

Given the dependency on x, we have

$$\partial_x^2 H_y = -k_x^2 H_y, \tag{1.19}$$

which finally gives

$$\partial_z^2 H_y + \left[\frac{\mu\varepsilon}{c^2} - k_x^2\right] H_y = 0. \tag{1.20}$$

The general solution in a given layer can thus be written

$$Hy = (A_j^+ e^{ik_z^j(z-z_j)} + B_j^+ e^{-ik_z^j(z-z_j)})e^{i(k_x x - \omega t)} \tag{1.21}$$

where $k_z^j = \sqrt{\mu_j\epsilon_j k^2 - k_x^2}$ where $k = \frac{\omega}{c} = \frac{2\pi}{\lambda}$. This expression means that in each layer two waves are present: a wave propagating upwards with an amplitude A_j^+ just under interface j, and a wave propagating downwards with an amplitude B_j^+ at the same place.

We could have taken, as a reference, the interface $j+1$ instead of j. In that case, the expression for H_y is

$$H_y = (A_j^- e^{ik_z^j(z-z_{j+1})} + B_j^- e^{-ik_z^j(z-z_{j+1})})e^{i(k_x x-\omega t)} \tag{1.22}$$

It is essential to mention that H_y is continuous owing to $\vec{rot}\vec{H}$ all throughout the structure. In addition, given the fact that the two expressions should be obviously equal for any value of x, z and t, the link between the coefficients is simply

$$B_j^- e^{+ik_z^i z_{i+1}} = B_j^+ e^{+jk_z^i z_i} \tag{1.23}$$

and

$$B_i^- = B_i^+ e^{ik_z^i k_i} \tag{1.24}$$

for the B coefficients, and for the A coefficients

$$A_j^- e^- ik_z^j z_{j+1} = A_j^+ e^{-jk_z^i z_i} \tag{1.25}$$

$$A_j^+ = A_j^- e^{+jk_z^i(z_i-z_{j+1})} = A_j^- e^{jk_z^j h_j}. \tag{1.26}$$

1.1.2 Boundary conditions

The fields that are parallel to the interfaces are continuous. In p polarization, this means that both H_y and E_x are continuous. For H_y, this condition yields, at the interface j located in z_j $A_{j-1}^- + B_{j-1}^- = A_j^+ + B_j^+$. And since

$$E_x = \frac{1}{i\omega\mu_0} \times \frac{\partial_z H_y}{\varepsilon}, \tag{1.27}$$

Then the quantity $\frac{\partial_z H_y}{\varepsilon}$ has to be continuous too, which yields

$$\frac{1}{\varepsilon_{j-1}} k_z^{j-1}(A_{j-1}^- - B_{j-1}^-) = \frac{1}{\varepsilon_j} k_z^j (A_j^+ - B_j^+) \tag{1.28}$$

We have then a system of equations, constituted by the two continuity equations written for each interface. The equations linking the A_j^+ and B_j^+ to the A_j^- and B_j^- must be added for each layer. However, solving the system directly doesn't work, because the numerical methods that are classically used prove to be unstable. We notice that the system is peculiar, since it links A_j and B_j with A_{j+1} and B_{j+1} and to A_{j-1} and B_{j-1} essentially, but not to the other coefficients. There are thus systematic ways to solve it, and one of these ways, the most stable, is to use scattering matrices, that we will explain now.

1.1.3 Scattering matrix algorithm

Interface scattering matrix

Consider the interface between medium j and $j+1$, the continuity of tangential component of the electric field vector $\vec{E}$ and normal component of the magnetic field $\vec{H}$ relations can be rewritten as follows

$$A_j^- + B_j^- = A_{j+1}^+ + B_{j+1}^+ \tag{1.29}$$

$$\frac{1}{\varepsilon_j} k_z^j (A_j^- - B_j^-) = \frac{1}{\varepsilon_{j+1}} k_z^{j+1} \left(A_{j+1}^+ - B_{j+1}^+\right) \tag{1.30}$$

Take A_j^- and B_{j+1}^+, then

$$A_j^- - B_{j+1}^+ = A_{j+1}^+ - B_j^- \tag{1.31}$$

and

$$\frac{k_z^j}{\varepsilon_j} A_j^- + \frac{k_z^{j+1}}{\varepsilon_{j+1}} B_{j+1}^+ = \frac{k_z^{j+1}}{\varepsilon_{j+1}} A_{j+1}^+ + \frac{k_z^j}{\varepsilon_j} B_j^- . \tag{1.32}$$

A few calculations lead to the following matrix form

$$\begin{bmatrix} A_j^- \\ B_{j+1}^+ \end{bmatrix} = \frac{1}{\frac{k_z^j}{\varepsilon_j} + \frac{k_z^{j+1}}{\varepsilon_{j+1}}} \begin{bmatrix} \frac{k_z^j}{\varepsilon_j} - \frac{k_z^{j+1}}{\varepsilon_{j+1}} & 2\frac{k_z^{j+1}}{\varepsilon_{j+1}} \\ 2\frac{k_z^j}{\varepsilon_j} & \frac{k_z^{j+1}}{\varepsilon_{j+1}} - \frac{k_z^j}{\varepsilon_j} \end{bmatrix} \begin{bmatrix} B_j^+ \\ A_{j+1}^- \end{bmatrix} \tag{1.33}$$

Layer matrix

Using expressions (1.24) and (1.26), a scattering matrix can be written for a layer

$$\begin{bmatrix} A_j^+ \\ B_i^- \end{bmatrix} = \begin{bmatrix} 0 & e^{ik_j h_j} \\ e^{ik_j h_j} & 0 \end{bmatrix} \begin{bmatrix} B_j^+ \\ A_j^- \end{bmatrix} \tag{1.34}$$

Cascading of scattering matrices

Once scattering matrices have been defined for interfaces and layers, they have to be assembled two by two to find the scattering matrix of the whole structure. The process is called cascading, and its main purpose is to obtain a single scattering matrix from two scattering matrices that concern partly the same variable. We assume we have coefficients A, B, C, D, E, F (that correspond to $A_j^{\pm}$ and$B_j^{\pm}$) that are linked by the following relations

$$\begin{bmatrix} A \\ B \end{bmatrix} = \begin{bmatrix} S_{11} & S_{12} \\ S_{21} & S_{22} \end{bmatrix} \begin{bmatrix} C \\ D \end{bmatrix} \tag{1.35}$$

$$\begin{bmatrix} D \\ E \end{bmatrix} = \begin{bmatrix} U_{11} & U_{12} \\ U_{21} & U_{22} \end{bmatrix} \begin{bmatrix} B \\ F \end{bmatrix} \tag{1.36}$$

We want to find a scattering matrix linking A and E to C and F, we therefore begin by eliminating the intermediate variables B and D using the straightforward results

$$B(1 - S_{22}U_{11}) = S_{21}C + S_{22}U_{12}F$$

and

$$D\,(1 - U_{11}S_{22}) = U_{11}S_{21}C + U_{12}F$$

So that A and E can be written

$$A = S_{11}C + \frac{S_{12}}{1 - U11S_{22}} \times [U_{11}S_{21}C + U_{12}F] \tag{1.37}$$

$$E = \frac{U_{21}S_{21}C}{1 - S_{22}U_{11}} + U_{12} + \frac{U21S_{22}U12}{1 - S_{22}U11}F \tag{1.38}$$

And finally, the scattering matrix linking A and E to C and F is

$$\begin{bmatrix} A \\ E \end{bmatrix} = \begin{bmatrix} S_{11} + \frac{S_{12}U_{11}S_{21}}{1-U_{11}S_{22}} & \frac{S_{12}U_{12}}{1-U_{11}S_{22}} \\ \frac{U_{21}S_{21}}{1-S_{22}U_{11}} & U_{22} + \frac{U_{21}S_{22}U_{12}}{1-S_{22}U_{11}} \end{bmatrix} \begin{bmatrix} C \\ F \end{bmatrix} \tag{1.39}$$

This formula can be used on any pair of scattering matrix provided each one of them has two coefficients (here B and D) in common. The matrices can be interface or layer matrices, or two matrices obtained through cascading.

1.1.4 Scattering matrix of the whole structure

Cascading all the interface and scattering matrices leads to the scattering matrix of the whole multilayered structure, whose coefficients are in fact directly the reflection and transmission coefficients of the whole structure, given the physical meaning of the amplitudes A_0, B_0, A_{N+1} and B_{N+1}.

$$\begin{bmatrix} B_0 \\ A_{N+1} \end{bmatrix} = \begin{bmatrix} r_1 & t_2 \\ t_1 & r_2 \end{bmatrix} \begin{bmatrix} A_0 \\ B_{N+1} \end{bmatrix} \tag{1.40}$$

Where r_1 is the reflection coefficient when a plane wave is coming from above. Using relations (1.37) and (1.38) it is possible to retrieve the intermediary coefficients, which means all the A_j and all the B_j. That way, it is possible to compute the field in each layer.

1.1.5 Examples

Although multilayered structures are a rather limited class of architectures, almost all the phenomenon of optics can be illustrated in this framework. By providing maps of the electric or magnetic fields, Moosh, a numerical swiss army knife for the study of the optical properties of multilayers[12]. Using Moosh, computing optical properties of any multilayered structure:

reflection, transmission, absorption spectra, as well as Gaussian beam propagation or guided modes, can be performed. In addition, Moosh allows to better grasp the physics – and this is what we will show here. We illustrate the capabilities of the method with several examples, of increasing complexity.

Refraction

That is why we begin with a phenomenon as simple as refraction. The picture shown Fig. 1.1 shows a beam refracted when encountering an interface between two media. The refracted beam and the reflected beam (producing a characteristic interference pattern) are clearly visible.

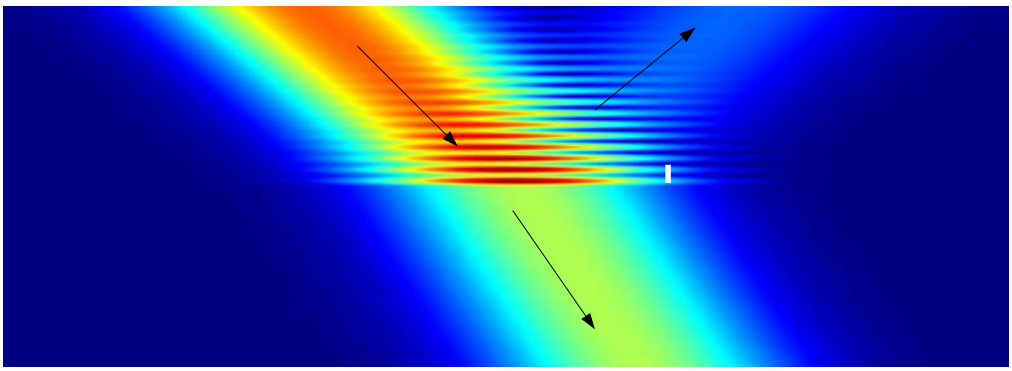


FIGURE 1.1: Refraction. Incident beam width of 10λ a wavelength of $\lambda = 800$nm, an angle of incidence=50° illuminating an interface air/dielectric of value 2 The overall width of the picture is 70λ and the height 25λ. The white bar represents one wavelength vertically (800 nm).

Brewster incidence

The reflection coefficient depends on the polarization of the incident light. In p polarization, the reflection coefficient presents a zero for a peculiar incidence angle called the Brewster angle (see Fig. 1.2). This "total transmission" can be simulated using Moosh, as shown on Fig. 1.3. There is still a very weak reflected beam, that is due to the fact that there are several plane

waves in the incident beam, so that the transmission can not be total, as some plane waves are slightly reflected.

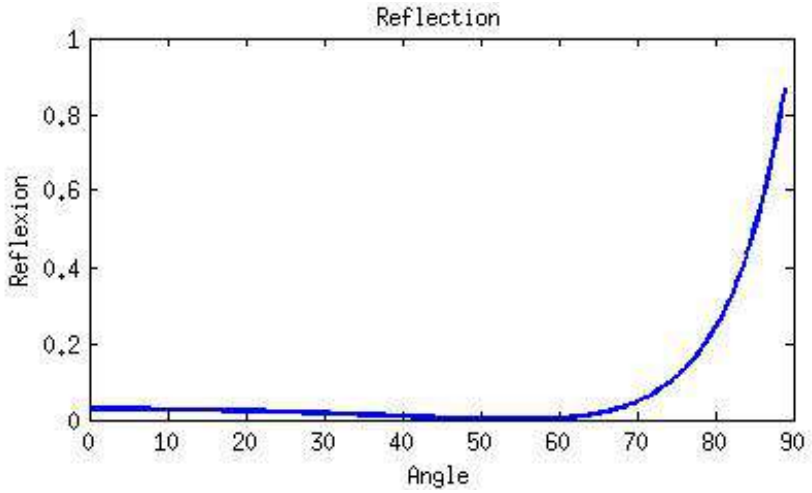


FIGURE 1.2: Reflection as a function of the incident angle with a wavelength of 600nm, number of points of 200 and number of periods = 20 of a dielectric value 2. The reflection coefficient reaches zero for an angle of 55°.

Total internal reflection

When a beam propagating in a high-index medium is sent on an interface with a lower index medium, total internal reflection occurs. While such a phenomenon is known even to high school students, Moosh allows to show what happens under the prism, and the evanescent wave that is generated. This is shown Figure 1.4

Anti-reflective coating

An anti-reflective coating is usually a quarter-wavelength layer of intermediate refractive index between air and the medium in which light is transmitted. Using Moosh, it is easy to compute both the transmission coefficient for different wavelength (see Fig. 1.5), and the propagation of the beam inside the structure(see Fig. 1.6), showing the resonance that allows light to be fully transmitted in normal incidence. Not interference pattern is present here, which shows how efficient the device is.

Bragg mirror

A Bragg mirror is a multilayer with two different indices with well chosen thicknesses. It is called a quarter-wave stack because each layer corresponds to a quarter of a wavelength in the medium (by taking into account the refractive index). Moosh allows to compute the reflection coefficient as a function of the wavelength, showing a range for which light is very efficiently

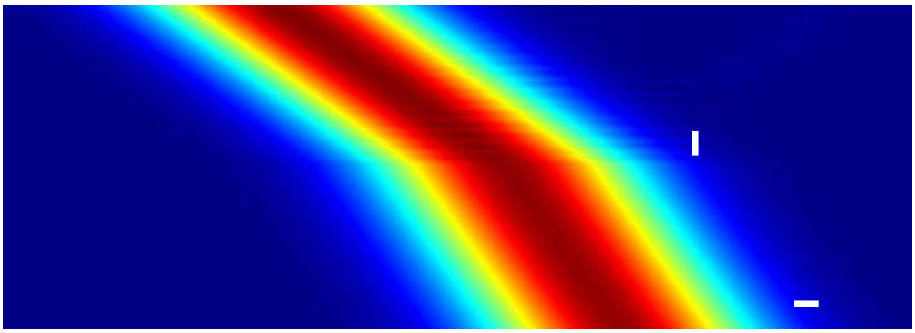


FIGURE 1.3: Brewster Incidence with a wavelength of 600nm. The white bar represents 1 wavelength.

reflected - this part is called the forbidden band, because light cannot propagate in the Bragg mirror for this wavelength range (see Fig. 1.7). Fig. 1.8 shows the reflection of a Gaussian beam.

Negative refraction

Negative refraction has been first predicted by V.g.Velasco in 1968[43]. But this fact didn't attract any attention at that time. In 2000, Smith et al. demonstrated the phenomenon of negative refraction experimentally[41]. MOOSH allows the study of such a process and the result is shown in Figure 1.3.

Perfect lensing

After the work of Smith, Pendry considered the device to be a perfect lens. Currently, Moosh is capable to study this phenomenon numerically, as shown Figure 1.10.

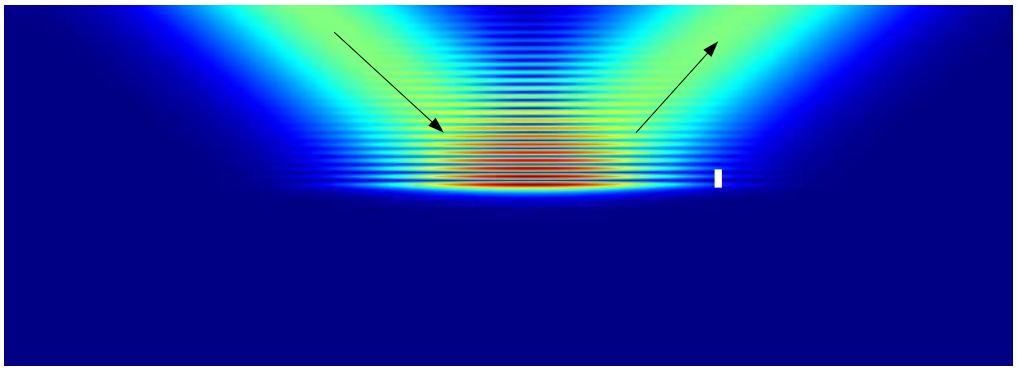


FIGURE 1.4: Total internal reflection, Incident beam width of 10λ a wavelength of $\lambda = 800$nm, an angle of incidence=50° illuminating an interface dielectric /air. The overall width of the picture is 70λ and the height 25λ.

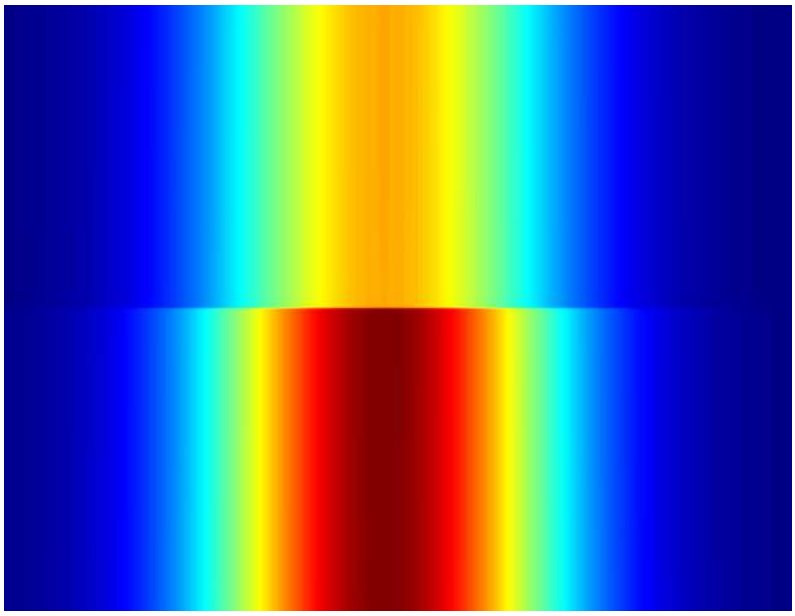


FIGURE 1.5: Anti Reflective Coating with a wavelength of 530nm, spatial window size $d = 70\lambda$, incident beam width $w = 10\lambda$ at normal incidence.

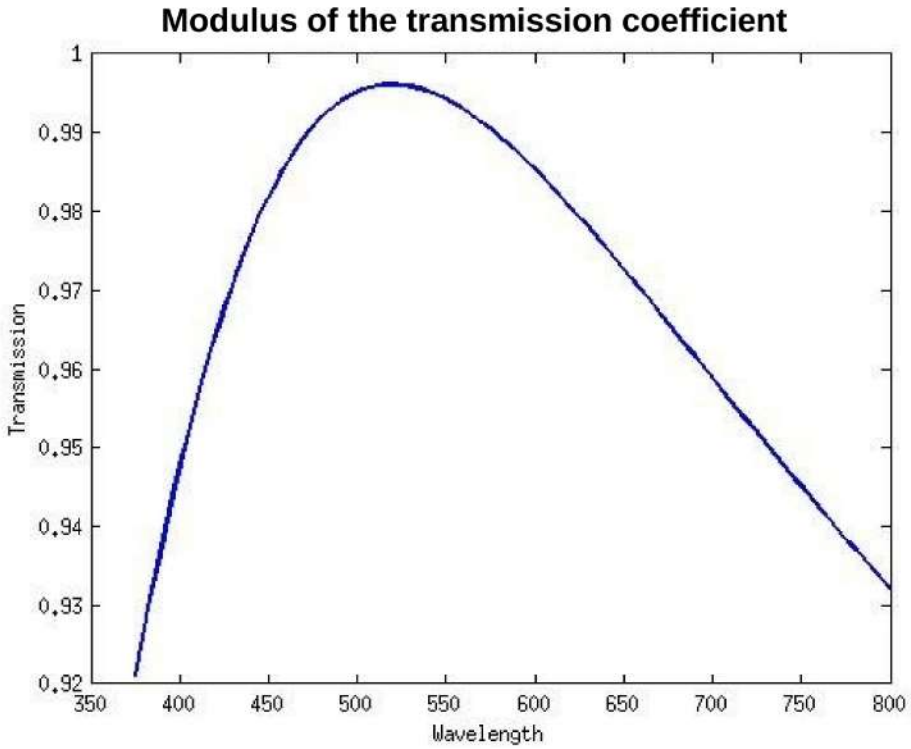


FIGURE 1.6: Transmission as a function of the wavelength with a spatial window size $d = 70\lambda$, incident beam width $w = 10\lambda$, and an angle of incidence of 45°.

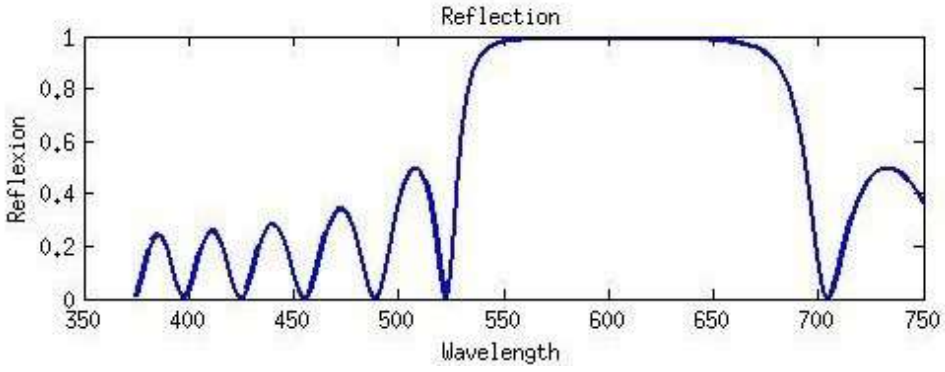


FIGURE 1.7: Bragg spectrum with a wavelength of 600nm, spatial window size $d = 70\lambda$, incident beam width $w = 10\lambda$, and an angle of incidence of 35°.

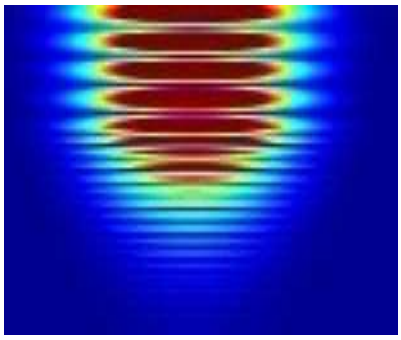


FIGURE 1.8: Bragg mirror.

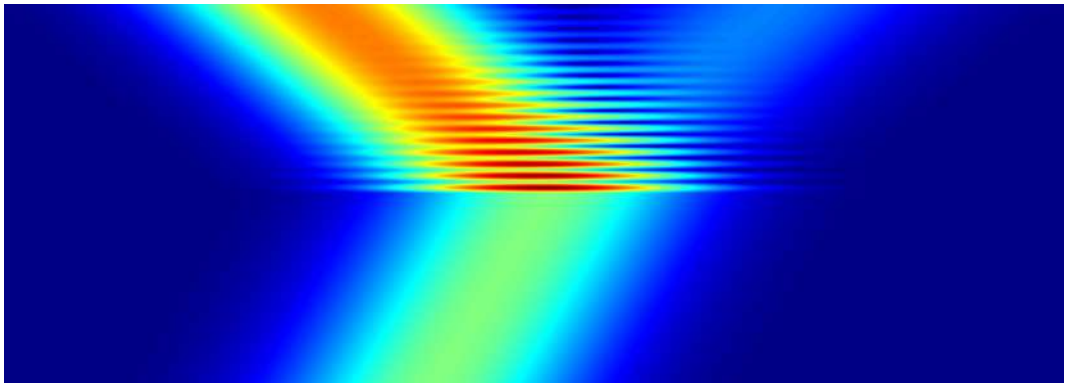


FIGURE 1.9: Negative refraction of a Gaussian beam with a waist of 50λ, $\lambda = 800nm$ propagating in air and meeting a slab of a negative index materials $\varepsilon = -2.25$, $\mu = 1$. The working wavelength is 363.8 nm, the incidence angle $75°$. The physical width of the domain is 15λ and the height 1965 nm.

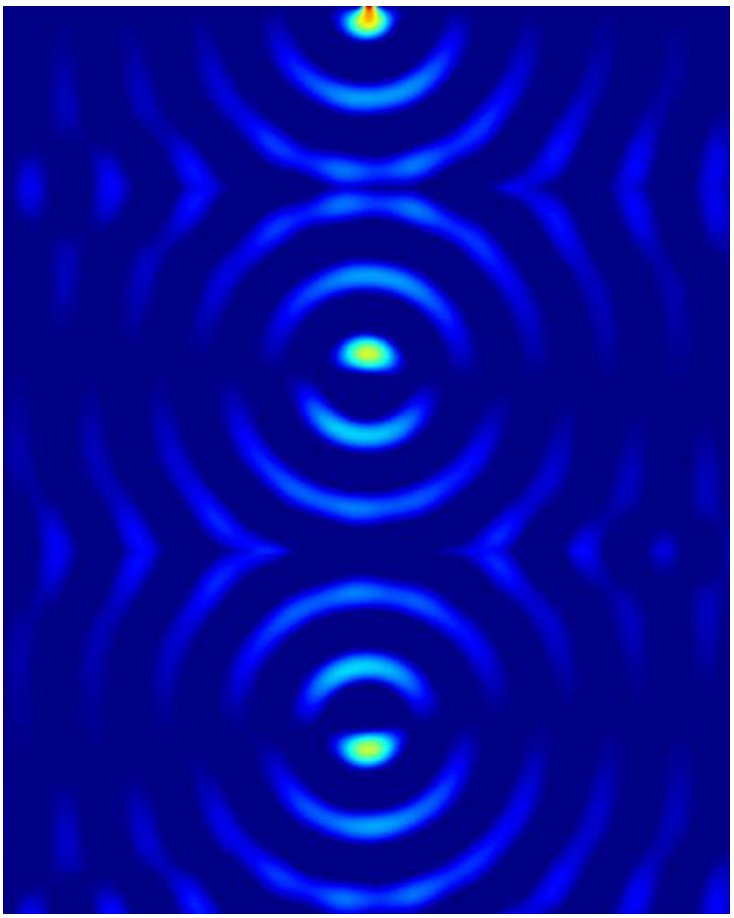


FIGURE 1.10: Perfect Lens. Incident beam width of 0.1λ a wavelength of $\lambda = 800$nm, illuminating an interface air/dielectric/air The overall width of the picture is 70λ and the height 25λ.

1.2 Guided modes

In plasmonics especially, guided modes play an essential role. Finding guided modes and computing their properties accurately is thus of great importance. A guided mode is a solution of Maxwell's equation without any incoming wave with boundary conditions, and as such, it only exists for very precise conditions.

When looking for guided modes, one assumes that

$$k_x > nk_0$$

where n is the maximum index of refraction of the outer media and $k_0 = \frac{\omega}{c}$. This means the fields present an exponential decay in the outside medium. It reduces to finding a solution to Maxwell's equations without any incoming wave from above or from under the structure. With N inside layers, the number of unknowns (2 by layer inside the structure, 1 for each outer medium) is $2N + 2$. It is exactly the number of equations of the type (1.29) and (1.30), since two can be obtained for each of the $N + 1$ interfaces.

Finally, the whole system of equations can be written under the form

$$M \begin{bmatrix} A_0 \\ A_1 \\ B_1 \\ \vdots \\ B_{N+1} \end{bmatrix} = 0.$$

The only way to get a solution that is not null is to have a singular matrix, which can be written

$$\det M = 0. \tag{1.41}$$

This relation provides the dispersion relation, that links the pulsation ω to the wave vector k_x and can be written, very generally

$$f(k_x, \omega) = 0.$$

However, using $\det M = 0$ proves unstable numerically and tedious when calculations have to be done by hand. In the latter case, the best solution is simply to take the whole system and eliminate all the unknowns one after the other. This yields a relation, at the end of the calculation, that is the dispersion relation.

Numerically, the equation $f(k_x, \omega) = 0$ must be solved in the complex plane in general. Once the frequency ω has been chosen, k_x is in general complex. A way to solve this equation is to look for minima of $|f(k_x, \omega)|$ instead of zeros of $f(k_x, \omega)$. Each minimum of $|f|$ is actually a zero of f, and $|f|$ does not present any other minimum than the zeros because f is a holomorphic function.

It is not always possible to find a dispersion relation by hand. Sometimes, this is too complicated and a purely numerical method is welcome.

This can be done in a stable way using scattering matrices. The scattering matrix of the whole multilayer is such that

$$\begin{bmatrix} A_0 \\ B_{N+1} \end{bmatrix} = [S] \begin{bmatrix} B_0 \\ A_{N+1} \end{bmatrix}$$

and looking for a guided mode, hence means looking for a solution for which

$$\begin{bmatrix} B_0 \\ A_{N+1} \end{bmatrix} = 0$$

but

$$\begin{bmatrix} A_0 \\ B_{N+1} \end{bmatrix} \neq 0$$

In other words, the problem can be written

$$[S]^{-1} \begin{bmatrix} A_0 \\ B_{N+1} \end{bmatrix} = 0$$

and here the dispersion relation is in that case simply

$$\det[S]^{-1} = 0,$$

which can be solved like explained above. S^{-1} must not be invertible and A_0 and $B_N + 1$ is the only solution.

1.3 Different light velocities

Now we concentrate on the question of the velocity of a guided mode.

1.3.1 Phase and group velocities

By definition, the phase velocity is the speed at which wave fronts (surfaces for which the phase presents the same value) travel. That is why it is called phase velocity. For a propagating mode, the phase velocity is thus simply given by the ratio

$$v_\phi = \frac{\omega}{k_x} \tag{1.42}$$

where ω is the angular frequency and k_x is the wave number.The direction of propagation is along the x axis.

The phase velocity is especially important for cavity resonances, because k_x and thus the effective wavelength $2\pi/k_x$ are what are critical for determining the right conditions to excite the resonance (frequency, angle...).

The group velocity by definition is the wave packet velocity of which the overall shape of the wave propagates through space. It is also defined as the velocity of transport in a dispersive medium.

$$v_g = \frac{\partial \omega}{\partial k_x} \tag{1.43}$$

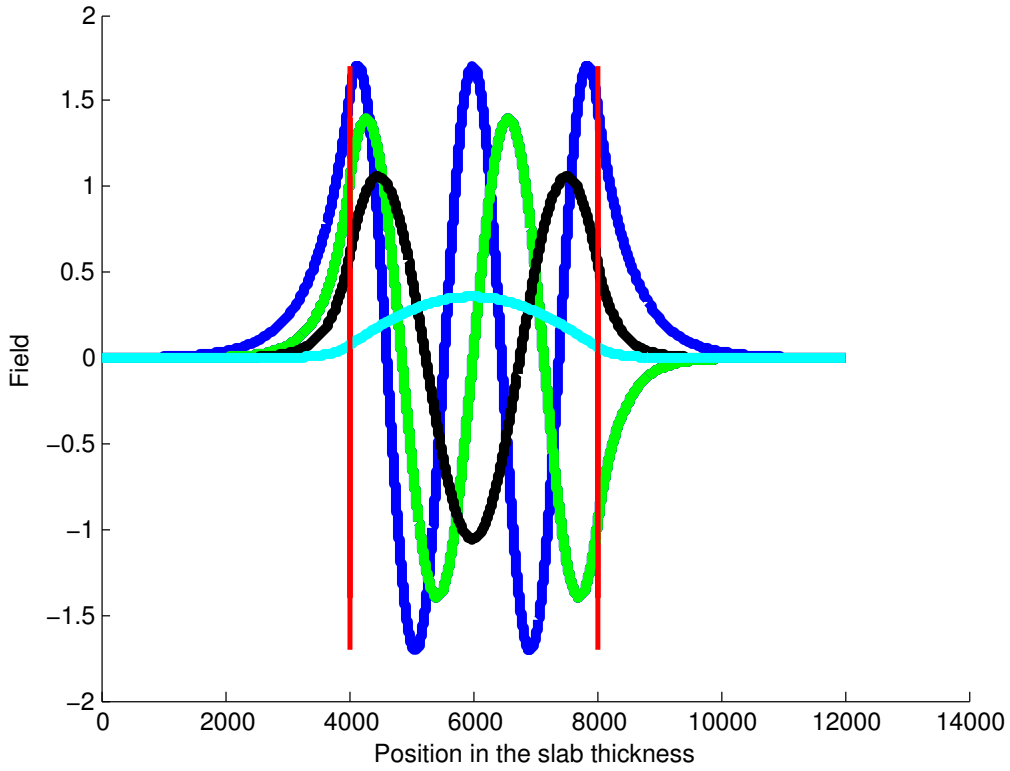


FIGURE 1.11: Guided Modes. Field profile (E_y), arbitrary units, for modes guided in a dielectric slab with a thickness of 1000 nm and a permittivity 4+0.1i (between the red lines) surrounded by a medium with a permittivity of 1 (air) for a wavelength of 700 nm.

We consider propagation in dielectric waveguides.

1.3.2 Energy velocity

The energy velocity, v_E has been recognized since a long time. Considering a wave of which the energy propagates with a certain velocity. This velocity is defined to be the velocity of the energy transport[8]. The energy velocity which can be defined as the ratio of the integral of the Poynting vector over the integral of the energy density

$$v_E = \frac{\int_{-\infty}^{+\infty} P_x dz}{\int_{-\infty}^{+\infty} \xi dz}. \tag{1.44}$$

Here the Poynting vector is actually the mean value of the actual Poynting vector, and since all the fields we are considering are complex, given the polarization we have

$$P_x = -\frac{1}{2}\Re E_z H_y^*. \tag{1.45}$$

The energy density we consider here is a mean value too[32], and it is given by

$$U = \frac{1}{4}\left(\mu_0\mu_r\vec{H}.\vec{H}^* + \varepsilon_0\varepsilon_r\vec{E}.\vec{E}^*\right). \tag{1.46}$$

In the non-dispersive and loss less case the energy velocity, v_E, has been proved to be equal to the group velocity, v_g by Yariv and Yeh[45]. Then

$$\frac{P}{U} = \frac{\partial\omega}{\partial k_x} \tag{1.47}$$

This means that:

$$v_E = v_g \tag{1.48}$$

Yariv and Yeh's original approach considers the matrix Bloch wave formalism in order to derive the dispersion behavior of electromagnetic modes layered periodic media[45].

Two variables are derived; the time averaged flux of energy in an electromagnetic field.

$$\vec{S} = \frac{1}{2}Re[\vec{E}\times\vec{H}^*]$$

and the time averaged electromagnetic energy density. It is given again by

$$U = \frac{1}{4}(\varepsilon|\vec{E}|^2 + \mu|\vec{H}|^2)$$

Both $\vec{S}$ and U are both periodic functions of x with a period **T**. It is better to define the space averaged quantities in a periodic medium. Thus the mean values over one period for U and $\vec{S}$ are given by

$$< U >= \frac{1}{\mathbf{T}}\int_0^T U(x)dx$$

and

$$< \vec{S} >= \frac{1}{\mathbf{T}}\int_0^T S(\vec{x})dx$$

The velocity of the energy flow or the energy velocity is

$$v_e = \frac{< S >}{< U >}$$

which gives the rate at which the energy flows from one cell to the next in a periodic medium.

The group velocity of a wave propagating in the same medium is proved to be equal to the energy velocity in this context too. The concepts of group, energy, and phase velocity in periodic systems are discussed in detail in the pioneering works of Yariv and Yeh[45] and[8].

Yariv and Yeh explained that their definitions are equivalent in systems

composed of non-absorbing materials[18], demonstrating that in this particular context we have

$$v_e = v_g \tag{1.49}$$

Although their result is established in the context of periodical structures, it can be easily extended to a single waveguide, as this is shown in Yeh's book[46].

The main consequence of this result is to make the energy velocity completely useless - because in the case of dielectrics there is no insight to get from the expression of v_E. What Yariv and Yeh have finally shown, is that there are two ways to derive the group velocity, one of them relying on the computation of the energy fluxes and densities in the structure.

As we will show in the following, this equality becomes much more interesting in plasmonics, when metals are involved. However, since metals are dispersive and contain electrons, the energy velocity is not even well defined and the theorem can not be extended without reconsidering the whole proof.

1.4 Conclusion

In this chapter, we have exposed the basics of how Maxwell's equations can be solved in the framework of multilayers, where the results are often analytic. The scattering matrix algorithm allows to solve the analytic systems of equations that can be found when writing the boundary conditions between two different layers.Scattering matrices numerically much more reliable in any condition than transfer matrix- that is why they were chosen for Moosh. And we have introduced all the concepts that will be used in the next chapters, insisting on the notion of velocity. Three different velocities can be defined: the phase (important for calculating resonance frequency in cavities), the group (the actual velocity of a signal) and the energy velocity. Yariv and Yeh's theorem shows that for guided modes just as for Bloch modes in Bragg mirrors, the last two velocities are simply equal. But in the context of dielectric materials the energy point of view does not really bring any useful insight, so that this theorem is largely ignored by the community and its demonstration quite hard to find[46].

Chapter 2

Plasmonics

Plasmonics is a domain of optics whose aim is to utilize metallic nanostructures to better control light. Metals play a particularly important role, as they allow to obtain very unusual light phenomena like negative refraction in multilayered structures, for instance. Metals actually provide an optical response to the incoming light that dielectrics are completely incapable of. A way of explaining why will be exposed in the next chapter.

Here we will introduce Drude's model, whose limitations will be discussed in Chapter 3, and the basic concepts of plasmonics, focusing especially on guided modes like surface plasmons and gap-plasmons.

It is worth underlining that plasmonics spans seemingly unrelated fields such as medicine (where plasmonics can be used for imaging[21], and gold nanoshells can be used in cancer treatment[24, 33], alternative energy (light concentrators for photovoltaics)[36] and integrated circuits (plasmonic interconnects)[3]. While not all these applications may be successful in the future, it underlines the wide potential of metallic nanostructures in different domains of Science.

Many analytic calculations are presented in this chapter. They may be sometimes tiresome, but in the beginning of my work, they constituted the only elements I could rely on to tell under which form Yariv and Yeh's theorem had a chance to be generalized. As will be shown in the next chapter, this is probably the simplest possible generalization, finally. But in the beginning, in order to know for instance if the energy conveyed by electrons had to be considered, we were using analytical calculations of the group velocity to guide us.

2.1 Drude's model

The most commonly used model for metal permittivity is the classical Drude model, developed by Paul Drude in 1900[13]. The model was derived in order to describe the optical properties of materials, especially metals, and it predicts with reasonable accuracy the permittivity and the conductivity of real metals by modeling the conduction-band electron motion in a metal lattice under an applied electric field. The Drude model considers a macroscopic point of view of charge carrier (an electron or a hole) motion, using a simple equation of motion and deriving the material permittivity in a harmonic oscillator.

In the Drude model, metals are considered as cloud of free electrons that are not bound to a particular atomic nucleus but are free to move within the metal lattice.

The central idea of Drude description of the optical response of metals is to consider that they can be described as dielectrics because the current can be considered as an effective polarization of the medium. This central idea is often overlooked, although it is very important – it can be used in any case, including for other models that link the electric field to the current in a more complicated way than Drude's model.

We call $\vec{P}$ the effective polarization and it is linked to the current by the following

$$\dot{\vec{P}} = \vec{J} \tag{2.1}$$

First, we show that the current can be easily included into Maxwell's equations. We start by Maxwell's first equation

$$\mathrm{div}\vec{E} = \frac{\rho}{\varepsilon_0}. \tag{2.2}$$

Since we have conservation of the charges, we have

$$\partial_t \rho + div\vec{J} = 0$$

which means that by replacing $\vec{J}$ we obtain

$$\partial_t \rho + div\partial_t \vec{P} = \partial_t \left(\rho + div\vec{P}\right) = 0.$$

In harmonic regime, and thus for any dynamic current, we have

$$\rho + div\vec{P} = 0$$

leading to

$$\rho = -div\vec{P}$$

It is then possible

$$div(\varepsilon_0 \vec{E} + \vec{P}) = 0$$

to introduce a $\vec{D} = \varepsilon_0 \vec{E} + \vec{P}$ vector, satisfying

$$div\vec{D} = 0$$

The same can be done with the following equation

$$\vec{rot}\vec{H} = \vec{J} + \varepsilon_0 \partial_t \vec{E},$$

using (2.1) so that we finally get

$$\vec{rot}\vec{H} = \partial_t \vec{D}.$$

This shows that the currents can actually be included, from Maxwell's equations point of view, as an effective polarization.

Now Drude'model makes a direct link between the electronic current and the electric field which pushes the electrons, by considering them as punctual particles pushed by the electric force. The current is in that case given by

$$\vec{J} = n(-e)\vec{v},$$

where n is the electron density, e the elementary charge and $\vec{v}$ the electron speed, so that we have

$$m_e\dot{\vec{v}} = (-e)\vec{E}$$

Finally, the relation between the effective polarization and the electric field is given by

$$\ddot{\vec{P}} = -ne\dot{\vec{v}}$$

$$\ddot{\vec{P}} = \frac{ne^2}{m}\vec{E}$$

where the electric field , $\vec{E} = \vec{E_0}\exp(-i\omega t)$ If we define the plasma frequency ω_p so that

$$\frac{ne^2}{m} = \varepsilon_0\omega_p^2$$

then we finally have a direct expression for the effective permittivity of metals

$$\varepsilon_m = 1 - \frac{\omega_p^2}{\omega^2} = 1 - \frac{\lambda^2}{\lambda_p^2} \tag{2.3}$$

ε_m is evaluated by the Drude Model. Starting with Newton's second law

The electric force:

$$\vec{F_e} = -e\vec{E}$$

and friction force:

$$\vec{f} = -\alpha\vec{v}$$

Solving the

$$-m\omega^2 x + j\alpha\omega x = -eE$$

then

$$x = \frac{\frac{eE}{m}}{\omega^2 - j\frac{\alpha}{m}\omega}$$

where

$$\tau = \frac{1}{\delta} = \frac{m}{\alpha}$$

$$\vec{P} = n\vec{p}$$

$$p = -ex$$

$$\vec{p} = \frac{-ne^2\frac{\vec{E}}{m}}{\omega^2 - j\frac{\omega}{\tau}}$$

Then

$$\vec{D} = \varepsilon_0(1 - \frac{\omega_p^2}{\omega^2 - j\omega\delta})\vec{E} \tag{2.4}$$

the plasma frequency ω_p is:

$$\omega_p^2 = \frac{ne^2}{m\varepsilon_0}$$

If the losses are neglected,

$$\varepsilon_r = 1 - \frac{\omega_p^2}{\omega^2}. \tag{2.5}$$

λ_p is the wavelength corresponding to the plasma frequency, typically 125 nm for noble metals as silver or gold. The model can be further refined by adding terms corresponding to the response of the background, considered as a dielectrics. These terms become important in the blue or UV region, where metals become absorbent because of the inter band transitions (transition between valence bands in metals, thus concerning bound electrons).

Using this simple model to describe the optical response of metals has allowed to better understand why metals would for instance reflect light so easily. The first thing that Drude's model brings in that framework is the notion of the skin depth, the typical penetration length for light in a metal, both on reflection and when guided modes are considered. This is shown on figure 2.1 using Moosh. When the metal is considered lossless, it is worth underlining that the skin depth is roughly constant, around 25 nm for noble metals.

2.2 Surface plasmons

Wood anomalies are absorption lines that appear when using metallic gratings to make spectra of white light. They were identified at the very beginning of the 20^{th} century[30] and explained by Fano[16] half a century later. Fano explained that a peculiar guided mode, the surface plasmon, propagating at the interface between the metal and the dielectric is excited by the grating, resulting in the absorption of the incoming light.

In the end of the 60's, these surface plasmons have been excited using two different setups based on prisms. These devices have been proposed by Otto[34] and Krestschman and Raether[20].

This guided mode is extremely important in plasmonics because most of the phenomena that occur in plasmonics can be linked, one way or the other, to the surface plasmon. In addition, the only well spread application

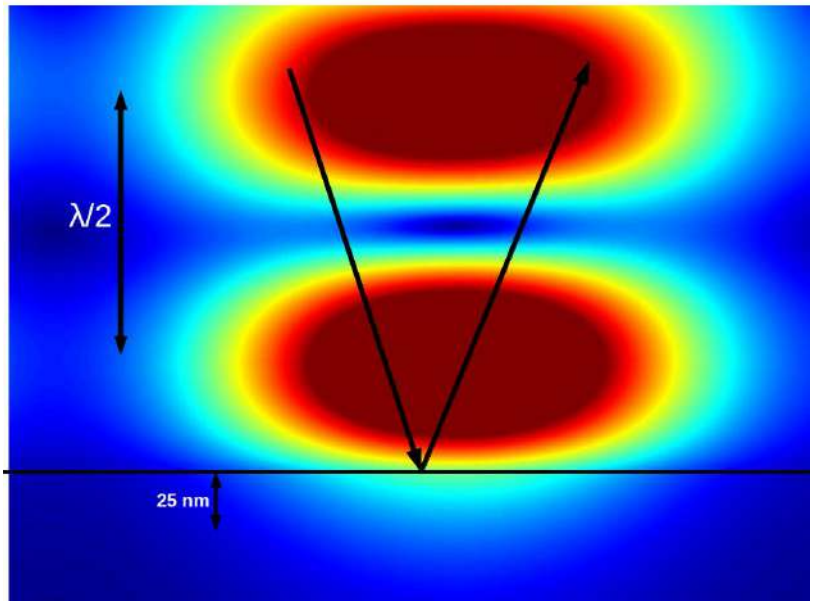


FIGURE 2.1: Skin Depth, Reflection of a plane wave with an incidence angle 70° with a spatial window size $d = 70\lambda$ and an incident beam of width $w = 10\lambda$.

of plasmonics so far is the detection of biological molecules using a prism coupler in the Kretschman Raether configuration.

2.2.1 Dispersion relation of the surface plasmon

Here, we will first derive the dispersion relation of the surface plasmon. The expressions of the fields in the dielectrics and in the metal respectively (for $y > 0$, in the dielectric)

$$H_y = A \exp(ik_x x) \exp(-\kappa_d z) \tag{2.6}$$

$$H_y = B \exp(-k_x x) \exp(\kappa_m z) \tag{2.7}$$

$$\kappa_m = \sqrt{k_x^2 - \varepsilon_m k_0^2} \tag{2.8}$$

and

$$\kappa_d = \sqrt{k_x^2 - \varepsilon_d k_0^2}. \tag{2.9}$$

Since we are looking for a guided mode in p polarization, we know that the H_y magnetic field in a dielectric and in a metal respectively are given by

$$H_y^d(x, z) = A \exp(ik_x x)\ \exp(-\kappa_d z) \tag{2.10}$$

for $y > 0$ in the dielectrics and

$$H_y^m(x, z) = B \exp(ik_x x) \exp(\kappa_m z) \tag{2.11}$$

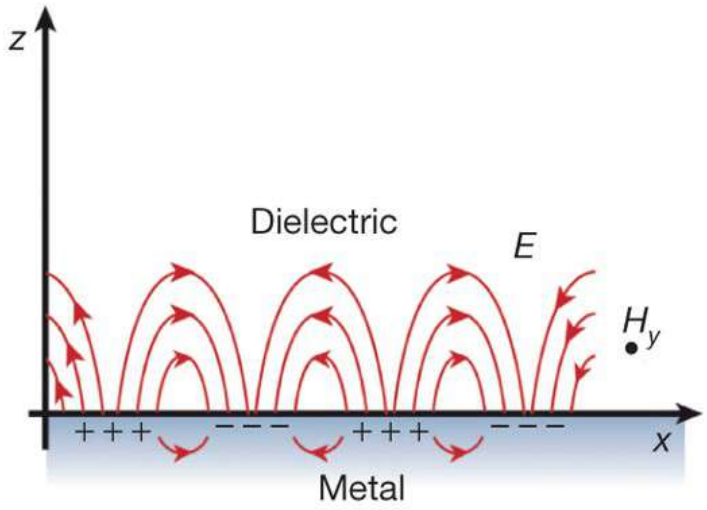


FIGURE 2.2: Surface plasmon. Taken from [4].

in the metal.

Two boundary conditions have then to be taken into consideration for y=0, and they are

$$H_y^m(x,0) = H_y^d(x,0) \tag{2.12}$$

and the second boundary condition, which must be satisfied whatever the values of x and for $y = 0$, is

$$\frac{1}{\varepsilon_m}\frac{\partial H_y^m}{\partial z} = \frac{1}{\varepsilon_d}\frac{\partial H_y^d}{\partial z} \tag{2.13}$$

which yields

$$\frac{\kappa_m}{\varepsilon_m} + \frac{\kappa_d}{\varepsilon_d} = 0, \tag{2.14}$$

the dispersion relation of the surface plasmon. In addition, by using the above expressions of κ_m and κ_d, the relationship between k_x, the surface plasmon wave vector, and ω can be put under the form

$$k_x = k_0\sqrt{\frac{\varepsilon_m\varepsilon_d}{\varepsilon_m + \varepsilon_d}} \tag{2.15}$$

provided $\varepsilon_m < 0$. As can be seen in this expression, it is even necessary that $|\kappa_m| > \kappa_d$ otherwise k_x is purely imaginary.

When taking into account the dispersive nature of metals, with Drude's model

$$\varepsilon_m = 1 - \frac{\omega^2}{\omega_p^2} = 1 - \frac{\lambda^2}{\lambda_p^2} \tag{2.16}$$

so that finally we have

$$k_x = k_0 \sqrt{\frac{1 - \frac{\lambda^2}{\lambda_p^2}}{\varepsilon_d + 1 - \frac{\lambda^2}{\lambda_p^2}}} \tag{2.17}$$

The dispersion has an asymptote when

$$k_x \to \infty$$

which occurs when

$$\lambda \to \frac{\lambda_p}{\sqrt{1 + \varepsilon_d}}$$

and finally when ω tends to

$$\omega_{sp} = \frac{\omega_p}{\sqrt{\varepsilon_d + 1}}$$

This shows that there is an asymptote for a peculiar frequency ω_{sp}, above which no surface plasmon can be excited.

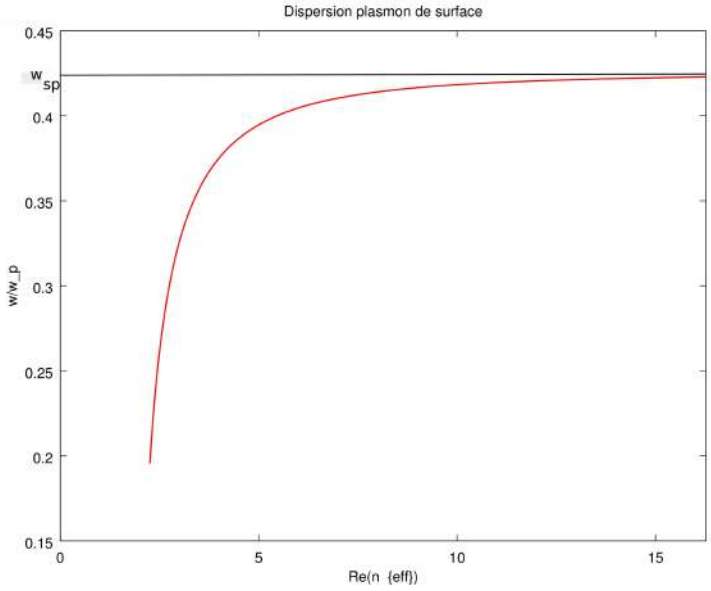


FIGURE 2.3: The dispersion relation of the Surface Plasmon, characterized by an asymptote for $\omega = \frac{\omega_p}{\sqrt{\varepsilon_d+1}}$, the frequency above which the surface plasmon cannot be excited. Losses do not change that point.

In reality, losses prevent the surface plasmon to reach very high wave vectors. The dispersion relation presents a bend-back relatively quickly, because ω_{sp} is in general in a frequency domain where inter band transition absorb light efficiently. Many theoretical studies neglect this however, because it is not always relevant to understand the fundamentals of the phenomena in plasmonics.

The asymptote is important because it means the surface plasmon is theoretically able to reach very high phase velocities around the surface plasmon frequency ω_{sp}. This is linked to very low group velocities, as will be explained in the next paragraph. Such a phenomenon is often called *slow light* and, as we will see, the surface plasmon is not the only mode for which it may occur.

2.2.2 Group velocity

As explained in the previous chapter, the group velocity of a guided mode is given by

$$v_g = \frac{\partial \omega}{\partial k_x}, \tag{2.18}$$

where k_x is the wave vector in the x direction. Here, we would like to see if Yariv and Yeh's prediction that the group velocity and the energy velocity are equal can be retrieved through direct calculations of both velocities in a simple case. The surface plasmon, with a non-dispersive metal, is the simplest case that can be imagined.

There are several ways to calculate the group velocity. The first way is by applying the above definition and derive the angular frequency by the wave number or, conversely, deriving the wave number with respect to the angular frequency and taking the inverse. This strategy works only in the case when ω is an explicit function of k_x (or the contrary). In general, the dispersion relation is too complicated for that strategy to be used.

Instead, since the dispersion relation can be written, very generally,

$$f(\omega, k_x) = 0. \tag{2.19}$$

We can write that

$$\mathrm{d}f = \frac{\partial f}{\partial k_x}\mathrm{d}k_x + \frac{\partial f}{\partial \omega}\mathrm{d}\omega \tag{2.20}$$

and if we follow a mode along its dispersion curve, then we should always have $\mathrm{d}f = 0$. This means that we have

$$\frac{\partial \omega}{\partial k_x} = -\frac{\frac{\partial \omega}{\partial k_x}}{\frac{\partial f}{\partial \omega}}. \tag{2.21}$$

Although the calculus is quite straightforward, the expression it yields is far from being simple. It is often not simple to use it to gain any physical intuition on the guided mode. In the case of the surface plasmon, the complexity is reasonable.

First, we try to find an expression of the group velocity in the non-dispersive case, in order to check Yariv and Yeh's theorem on a practical example involving (non-dispersive) metals

$$\frac{\partial f}{\partial k_x} = \frac{1}{\varepsilon_m}\frac{\partial \kappa_m}{\partial k_x} + \frac{1}{\varepsilon_d}\frac{\partial \kappa_d}{\partial k_x} = \frac{k_x(\varepsilon_m\kappa_m + \varepsilon_d\kappa_d)}{\varepsilon_m\varepsilon_d\kappa_m\kappa_d} \tag{2.22}$$

and

$$\frac{\partial f}{\partial \omega} = \frac{1}{\varepsilon_m}\frac{\partial \kappa_m}{\partial \omega} + \frac{1}{\varepsilon_d}\frac{\partial \kappa_d}{\partial \omega} = -\frac{\omega}{c^2}\frac{\kappa_m + \kappa_d}{\kappa_m \kappa_d}. \tag{2.23}$$

Then, after quite a few simplifications, we get

$$v_g = \frac{k_x \omega(\varepsilon_m \kappa_m + \varepsilon_d \kappa_d)}{k_0^2 \varepsilon_m \varepsilon_m (\kappa_m + \kappa_d)}. \tag{2.24}$$

Substituting k_0 by $\frac{\omega}{c}$ in equation (2.24), we obtain

$$v_g = \frac{\omega(\varepsilon_m \kappa_m + \varepsilon_d \kappa_d)}{k_x(\varepsilon_m + \varepsilon_d)(\kappa_m + \kappa_d)} \tag{2.25}$$

From the dispersion relation of the surface plasmon we know that

$$\varepsilon_m \kappa_d + \varepsilon_d \kappa_m = 0 \tag{2.26}$$

so that finally, in the non-dispersive case, it is possible to write

$$v_g = v_\phi = \frac{\omega}{k_x}. \tag{2.27}$$

2.2.3 Energy velocity

In order to evaluate the energy velocity of a surface plasmon, two parameters should be evaluated: the Poynting vector flux which is denoted by π_x and the mean energy density which is denoted by ξ. In the non-dispersive case this can be easily done.

$$v_E = \frac{\int_{-\infty}^{+\infty} \pi_x dz}{\int_{-\infty}^{+\infty} \xi dz} \tag{2.28}$$

The Poynting vector in the x direction in the metal and the dielectric will be denoted π_m and π_d respectively. We have

$$\pi_x^m = \frac{k_x |A|^2 H_y H_y^*}{2\omega \varepsilon_0 \varepsilon_m} \tag{2.29}$$

$$\pi_x^d = \frac{k_x |A|^2 H_y H_y^*}{2\omega \varepsilon_0 \varepsilon_d} \tag{2.30}$$

and since $H_y H_y^* = \exp(-2\kappa_m z)$ in the metal, or $H_y H_y^* = \exp(-2\kappa_d z)$ in the dielectric.

$$\pi_x^m = \frac{k_x |A|^2 \exp(-2\kappa_m z)}{2\omega \varepsilon_0 \varepsilon_m} \tag{2.31}$$

and

$$\pi_x^d = \frac{k_x |A|^2 \exp(-2\kappa_d z)}{2\omega \varepsilon_0 \varepsilon_d} \tag{2.32}$$

Integrating the Poynting flux gives

$$\int_{-\infty}^{+\infty} \pi_x dz = \int_{-\infty}^{0} \pi_x^m dz + \int_{0}^{+\infty} \pi_x^d dz \tag{2.33}$$

$$\int_{-\infty}^{0} \pi_x^m dz = \frac{k_x |A|^2}{4\kappa_m \omega \varepsilon_0 \varepsilon_m} \tag{2.34}$$

$$\int_{0}^{+\infty} \pi_x^d dz = \frac{k_x |A|^2}{4\kappa_d \omega \varepsilon_0 \varepsilon_d} \tag{2.35}$$

| A | =1, then

$$\int_{-\infty}^{+\infty} \pi_x dz = \frac{k_x(\kappa_m \varepsilon_m + \kappa_d \varepsilon_d)}{4\omega \varepsilon_0 \kappa_m \kappa_d \varepsilon_m \varepsilon_d} \tag{2.36}$$

By simplification

$$\int_{-\infty}^{+\infty} \pi_x dz = \frac{k_x}{4\omega\varepsilon_0} \left(\frac{1}{\varepsilon_m \kappa_m} + \frac{1}{\varepsilon_d \kappa_d} \right) \tag{2.37}$$

The Energy density is denoted by ξ here and we assume its expression to be simply

$$\xi = \frac{1}{2} \left(\frac{1}{2} \mu_0 |H_y|^2 + \frac{1}{2} \varepsilon_0 \varepsilon \vec{E}.\vec{E^*} \right) \tag{2.38}$$

and since

$$E_x E_x^* = \frac{\kappa_d^2 \exp(-2\kappa_d z)|A|^2}{\omega \varepsilon_0^2 \varepsilon_d^2} \tag{2.39}$$

and

$$E_z E_z^* = \frac{k_x^2 \exp(-2\kappa_d z)|A|^2}{\omega^2 \varepsilon_0^2 \varepsilon_d^2} \tag{2.40}$$

we finally obtain

$$\xi_d = \frac{1}{4}\mu_0 |A|^2 \exp(-2\kappa_d z) + \frac{1}{4} \frac{1}{\omega^2 \varepsilon_0 \varepsilon_d} [\kappa_d^2 + k_x^2] |A|^2 \exp(-2\kappa_d z) \tag{2.41}$$

where $\kappa_d^2 = k_x^2 - \varepsilon_d k_0^2$. The next step is then

$$\xi_d = \frac{1}{4}\mu_0 |A|^2 \exp(-2\kappa_d z) + \frac{1}{4} \frac{1}{\omega^2 \varepsilon_0 \varepsilon_d} [2k_x^2 - \varepsilon_d \omega^2 \varepsilon_0 \mu_0] |A|^2 \exp(-2\kappa_d z). \tag{2.42}$$

Upon simplification, using that $k_0^2 = \omega^2 \varepsilon_0 \mu_0$ we obtain

$$\xi_d = \frac{k_x^2}{2\omega^2 \varepsilon_0 \varepsilon_d} |A|^2 \exp(-2\kappa_d z) \tag{2.43}$$

By integrating the energy density we have in the dielectric

$$\int_0^{+\infty} \xi_d dz = \frac{k_x^2}{4\omega^2 \varepsilon_0 \varepsilon_d \kappa_d} \tag{2.44}$$

and in the metal

$$\int_{-\infty}^{0} \xi_m dz = \frac{k_x^2}{4\omega^2 \varepsilon_0 \varepsilon_m \kappa_m} \tag{2.45}$$

Now the two flux must be added. Adding equations 2.46 and 2.47 gives the integral of the energy density

$$\int_{-\infty}^{+\infty} \xi dz = \int_{-\infty}^{0} \xi_m dz + \int_0^{+\infty} \xi_d dz. \tag{2.46}$$

The resulting expression is

$$\int_{-\infty}^{+\infty} \xi dz = \frac{k_x^2}{4\omega^2 \varepsilon_0} \left(\frac{1}{\varepsilon_d \kappa_d} + \frac{1}{\varepsilon_m \kappa_m} \right). \tag{2.47}$$

In order to evaluate the energy velocity , calculating equation 2.28, The ratio of equation 2.36 and equation 2.46 gives

$$v_E = \frac{\int_{-\infty}^{+\infty} \pi_x dz}{\int_{-\infty}^{+\infty} \xi dz} = \frac{\omega}{k_x} \tag{2.48}$$

Then in the non dispersive case, for a surface plasmon, we can thus see that the theorem holds and that we have

$$v_E = v_g \tag{2.49}$$

This may look as a trivial result, but this shows that even in the case of a (non-dispersive) metal Yariv and Yeh's theorem can be applied to the surface plasmon without having to consider the kinetic energy of the electron gas in the energy density, nor in the energy flux.

2.2.4 Dispersive case

In the dispersive case, the group velocity can be calculated too, but it cannot be compared to the energy velocity as it is not obvious what expression should be chosen for the energy density.

Starting with the dispersion relation of Surface plasmons:

$$\frac{\kappa_m}{\varepsilon_m} + \frac{\kappa_d}{\varepsilon_d} = 0 \tag{2.50}$$

$$v_g = -\frac{\frac{\partial f}{\partial k_x}}{\frac{\partial f}{\partial \omega}} \tag{2.51}$$

$$\frac{\partial f}{\partial k_x} = \frac{1}{\varepsilon_m}\frac{\partial \kappa_m}{\partial k_x} + \frac{1}{\varepsilon_d}\frac{\partial \kappa_d}{\partial k_x} \tag{2.52}$$

$$\frac{1}{\varepsilon_m}\frac{\partial \kappa_m}{\partial k_x} = \frac{k_x}{\varepsilon_m \kappa_m}$$

$$\frac{1}{\varepsilon_d}\frac{\partial \kappa_d}{\partial k_x} = \frac{k_x}{\varepsilon_d \kappa_d}$$

$$\frac{\partial f}{\partial k_x} = \frac{k_x(\varepsilon_d\kappa_d + \varepsilon_m\kappa_m)}{\varepsilon_m\varepsilon_d\kappa_m\kappa_d} \tag{2.53}$$

$$\frac{\partial f}{\partial \omega} = \frac{\varepsilon_m \frac{\partial \kappa_m}{\partial \omega} - \kappa_m \frac{\partial \varepsilon_m}{\partial \omega}}{\varepsilon_m^2} + \frac{1}{\varepsilon_d}\frac{\partial \kappa_d}{\partial \omega} \tag{2.54}$$

$$\varepsilon_m \frac{\partial \kappa_m}{\partial \omega} = \frac{-k_0\varepsilon_m}{\sqrt{k_x^2c^2 - \omega^2 + \omega_p^2}}$$

$$\kappa_m \frac{\partial \varepsilon_m}{\partial \omega} = \frac{2\omega_p^2\kappa_m}{\omega^3}$$

$$\frac{1}{\varepsilon_d}\frac{\partial \kappa_d}{\partial \omega} = \frac{1}{\varepsilon_d}\frac{-k_0\varepsilon_d}{\sqrt{k_x^2c^2 - \varepsilon_d\omega^2}} = \frac{-k_0}{\sqrt{k_x^2c^2 - \varepsilon_d\omega^2}}$$

Solving the above equations gives

$$\frac{\partial f}{\partial \omega} = \frac{-k_0\varepsilon_m\omega^2 H - 2GH\kappa_m\omega_p^2 - \kappa_0 G\varepsilon_m^2\omega^2}{GH\varepsilon^2\omega^2} \tag{2.55}$$

where

$$G = \sqrt{k_x^2c^2 - \omega^2 + \omega_p^2}$$

and

$$H = \sqrt{k_x^2c^2 - \varepsilon_d\omega^2}$$

Solving equation 2.44 gives the expression of the group velocity

$$v_g = \frac{k_x(\varepsilon_d\kappa_d - \varepsilon_m\kappa_m)(GH\varepsilon_m^2\omega^2)}{(\varepsilon_m\varepsilon_d\kappa_m\kappa_d)(k_x\varepsilon_m\omega^2 H - 2GH\kappa_m\omega_p^2 - +k_0 G\varepsilon_m^2\omega^2)} \tag{2.56}$$

The form taken by this group velocity is such that it is hardly intelligible. It is thus difficult to interpret and use to form ones intuition on the behavior of the mode. It is not obvious, from the above expression, that Yariv and Yeh's theorem holds - which was our hope here.

2.3 Prism couplers

In a multilayered structure illuminated from above, since k_x is conserved throughout the whole structure, we can expect a surface plasmon to be excited when the incident wave presents a wave vector k_x that is given by 2.15. It is thus not possible to excite a surface plasmon using a propagating beam

coming directly from the dielectric supporting the guided mode. The wave-vectors k_x of the different plan waves that are involved have a k_x that will always be smaller than k_0. They cannot excite the mode in that condition, because its effective index is larger than 1. In order to generate k_x vectors that are larger, a prism can be used because the wave-vector along the x direction of a plane wave is in that case given by

$$k_x = n\, k_0 \sin\theta \tag{2.57}$$

and if the index n is larger than the index of the dielectric at the interface of which the surface plasmon propagates, then a surface plasmon can theoretically be excited. In order to do so, the k_x that is sent has to satisfy roughly

$$k_x \simeq k_{sp} \tag{2.58}$$

which can be written

$$n \sin\theta \simeq \sqrt{\frac{\varepsilon_d \varepsilon_m}{\varepsilon_d\, \varepsilon_m}}. \tag{2.59}$$

The difference between the theoretical angle for which the surface plasmon can be excited and the actual one is due to the fact that the guided mode is disturbed by the prism and becomes a leaky mode.

Two configurations have thus been proposed, both using a prism to generate a high enough wave vector. The first configuration has been published by Otto[34] in 1968 and marks the beginning of plasmonics as a field.

In the Otto configuration, the prism is simply placed above the surface of the metal. The surface plasmon is simply excited when the light inside the prism has an incidence angle larger than the critical angle and satisfying the resonance condition above. This case has been simulated using Moosh and the resulting magnetic field map is shown in figure 2.5. The surface plasmon excited at the interface between the metal and air can very clearly be seen here.

In order to illustrate that the surface plasmon can excited only if the resonance condition is respected, the reflection coefficient is shown, as a function of the angle, on figure 2.7.

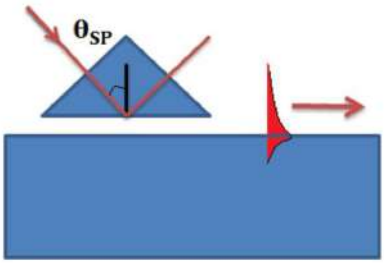


FIGURE 2.4: Otto Configuration

The second configuration, proposed by Kretschmann and Raether[19] in 1972, is actually the most used, for practical reasons. In the Kretschmann-Raether (KR) configuration, the metal film is evaporated on top of a glass prism, as shown in figure 2.8. Then the film is illuminated through the dielectric prism at an angle of incidence greater than of total internal reflection angle satisfying the excitation condition.

Exactly as for the Otto configuration, when the right angle of incidence is chosen, a surface plasmon resonance is excited. The profile of the magnetic field in such a case, computed using Moosh, is shown in figure 2.9.

2.3.1 SPR bio-sensors

The only, so far, commercial application of plasmonics is biosensing. The principle is to use a Kretschmann-Raether configuration composed of a light source, prism attached to a thin gold film and a detector. At the resonance angle, the surface plasmon is excited - but the very angle for which this happens depends on the state of the lower surface (see Figure 2.10). This surface is functionalized: organic molecules are binded to the gold surface, ready to bind themselves to the free molecules that are in the liquid below the metallic surface. As this molecular binding occurs, there will be a shift

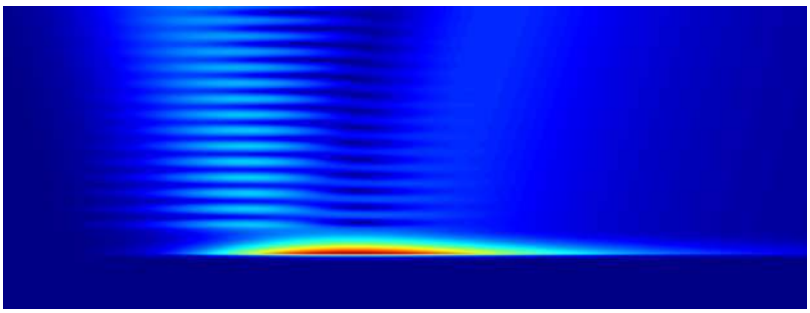


FIGURE 2.5: Otto configuration with a wavelength of 600 nm, the spatial window size is 150λ, the incident beam width is 10λ, and the critical angle 44.9°

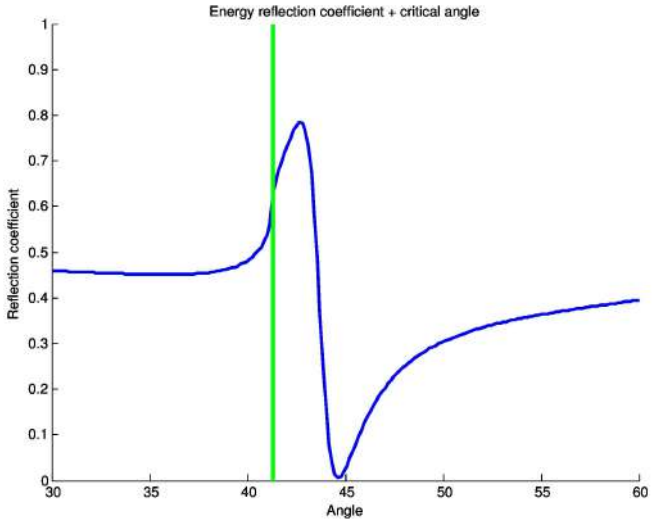


FIGURE 2.6: Surface Plasmon Resonance

in the reflectivity curve i.e. a shift in resonance. The KR configuration has the advantage that it is easy to change the liquid in contact with the metallic surface or to introduce new molecules to analyze, which is not the case with the Otto configuration.

Figure 2.10 illustrates the principle of the SPR sensing.

Using Moosh, the reflection coefficient as a function of the angle can be computed for a SPR when the metal is covered by a very thin dielectric film, representing the binded molecules of interest. Figure 2.11 shows the result for different layer thicknesses. Classically, the index of the layer is considered to be around 1.46 (typical of organic materials) and its thickness of a few nanometers (3 nm is often taken in the literature to test the sensitivity of a device).

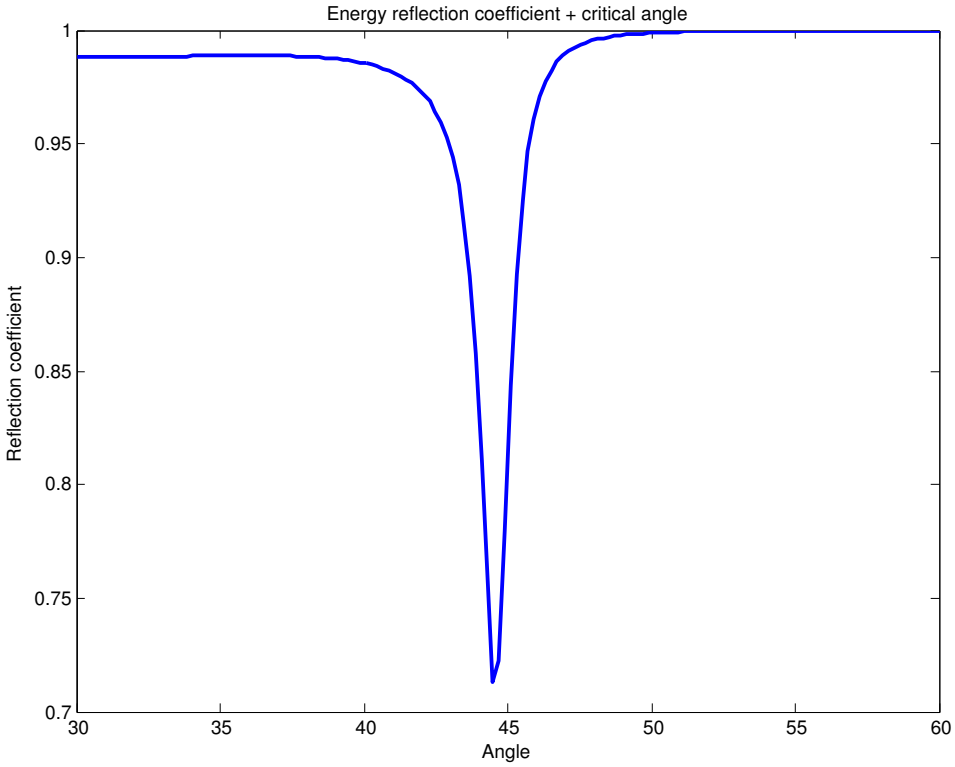


FIGURE 2.7: Reflection as a function of the critical angle with a wavelength of 600 nm, the spatial window size is 150λ, the incident beam width is 10λ,and the critical angle 44.9 °

2.4 Metallo-dielectrics

Metallic slabs have been considered as a sort of lens [35], mainly because they support surface plasmons that allow to convey the information usually contained in evanescent, thanks to their property to propagate evanescent, somehow, not far angularly speaking from the surface plasmon resonance.

More importantly, metallo dielectric[40] are able to transmit light although they contain a lot of metal, as if the dielectric was able to help the light tunneling through. Another way to see that : metallo-dielectric present band structures that can be hyperbolic[42] and thus lead to negative refraction. Such an effect has actually been largely observed[44] and even used to enhance the resolution of some peculiar lenses.

Essentially, a periodic metallo-dielectric multilayer is characterized by solely the thickness d_m of metallic layers and the thickness d_d of dielectric layers. The metallic filling ratio is defined by

$$\rho = \frac{d_m}{d_m + d_d}. \tag{2.60}$$

Such a structure has a dispersion relation that is similar to the one of Bragg mirrors. When the wavelength of light becomes large compared to the period $d = d_m + d_d$ then the medium behaves as an homogeneous

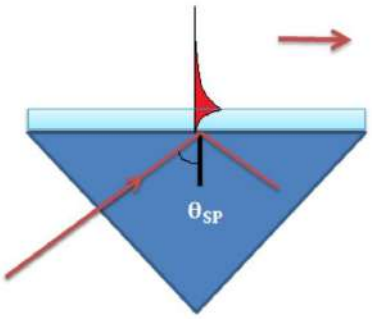


FIGURE 2.8: Kretschmann Configuration

medium for light - but it is anisotropic. More precisely, the dispersion relation for p polarized light, in that limit, becomes[37]

$$\frac{k_x^2 + k_y^2}{\varepsilon_\parallel} + \frac{k_z}{\varepsilon_\perp} = \frac{\omega^2}{c^2}, \tag{2.61}$$

with

$$\varepsilon_\parallel = \frac{\varepsilon_m \varepsilon_d}{\rho\varepsilon_m + (1-\rho)\varepsilon_d}. \tag{2.62}$$

Because of the dispersive nature of metals, both effective permittivities change with the frequency. When the filling ratio is high enough, two phenomenon can occur.

When $\varepsilon_\parallel$ becomes negative, while $\varepsilon_\perp > 0$ obviously the dispersion relation, instead of being an ellipsoid, becomes an hyperbole (shown figure 2.12). It is not possible to have $k_z = 0$, the dispersion relation cannot be satisfied in that case. This produces negative refraction[5], even if this is not always easy to identify[44]. Such a phenomenon is easy to simulate with Moosh (see figure 2.13). This case is called Type I hyperbolic meta material.

When on the contrary, $\varepsilon_\perp < 0$ and $\varepsilon_\parallel > 0$, $k_x = k_y = 0$ is not possible any more and the hyperboloid is completely different. This usually means that

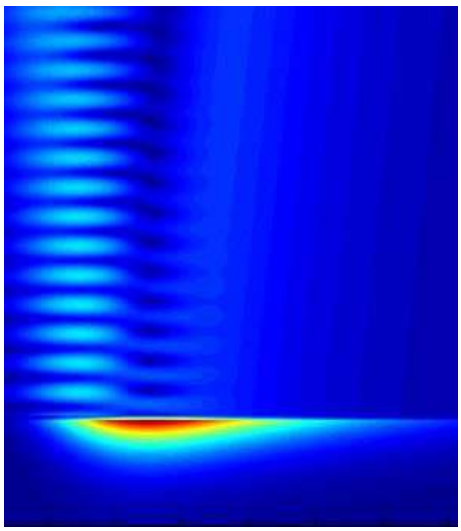


FIGURE 2.9: Kretschmann Raether configuration with a wavelength of 630 nm,spatial window size $d = 150\lambda$ and an incident beam width $w = 10\lambda$ and an angle of incidence of 44.935°

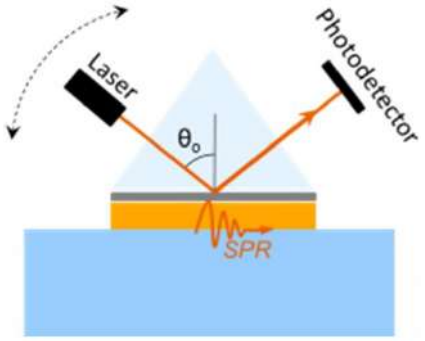


FIGURE 2.10: Biosensing using a Kretschmann-Raether configuration.

nothing propagates when coming from outside in the medium, if the wave vector along the x axis is not high enough. But such meta materials support very high effective index guided modes, similar to gap-plasmons (see next section).

2.5 Gap-plasmons

A gap-plasmon is the fundamental mode of Metal Insulator-Metal waveguide with a thickness of the insulator less than 50 nm in the visible. This is roughly twice the skin depth and the next chapter will definitely help to understand why this peculiar thickness. When such a gap is constituted in a metallic structure, then resonances appear that can be linked to the excitation of a gap-plasmon.

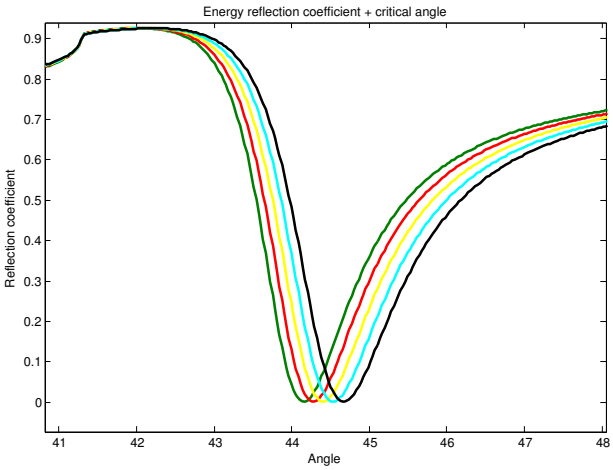


FIGURE 2.11: Kretschmann-Raether Configuration,Gap plasmon. Energy coefficient as a function of the incidence angle for several thicknesses of the layer on top of gold from 0 to 5 nm, with an index of 1.46, typical of organic materials.

The first paper published about a gap-plasmon resonator was written by Leveque and Martin[23]. They studied the resonance arising when a flat nanoparticle is coupled to a thin gold film. In their article, Leveque and Martin, recognized that the field along the interface reaches its maximum under the particle and follows a law in $d^{-3/2}$ where d is the distance between the particle and the film. Leveque and Martin, using numerical simulations, have predicted an electric field intensity enhancement of 5000 for the Localized Surface Plasmons (LSP) resonance with $\lambda = 600nm$ and a gap of $d = 5nm$. However, they did not really perform any physical analysis beyond their calculations.

Gap plasmons have been well understood in the study performed by Sergey I. Bozhevolnyi and Thomas Søndergaard in 2007 [7]. They have explained that the gap-plasmon propagating under the particle considered the film coupled particle as a cavity, which explains the concentration of electromagnetic energies into sub wavelength volumes and the enhancement of both scattered and local electric fields. They called the structures metal-insulator-metal (MIM).

The gap-plasmon has an effective index $n_{gp} = \frac{k_x}{k_0}$ that diverges when the width of the gap tends to zero. Theoretically, there is thus no limit to the effective index of the mode. Practically, the effective index never goes beyond 10 - many other phenomena, as spatial dispersion, hinder the gap-plasmon to reach an extremely high effective index.

A patch constitutes a cavity for the gap-plasmon because it is reflected by the edges of the patch. Consequently, the typical size of cavity d for a gap-plasmon is given, for the fundamental mode by

$$d = \frac{\lambda_0}{2n_{gp}}. \tag{2.63}$$

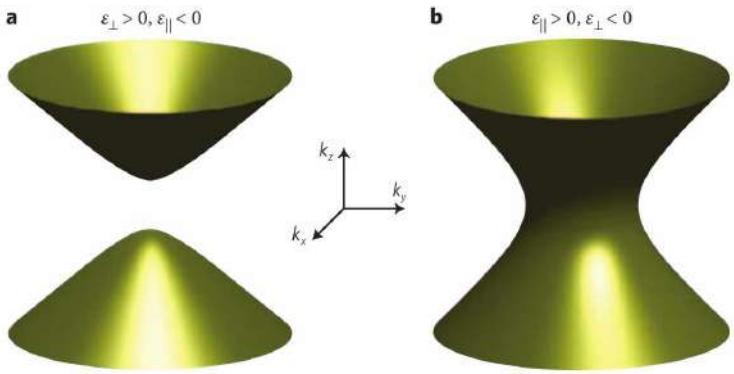


FIGURE 2.12: Figure taken from [37] illustrating the dispersion properties of hyperbolic meta materials in the wave vector space.

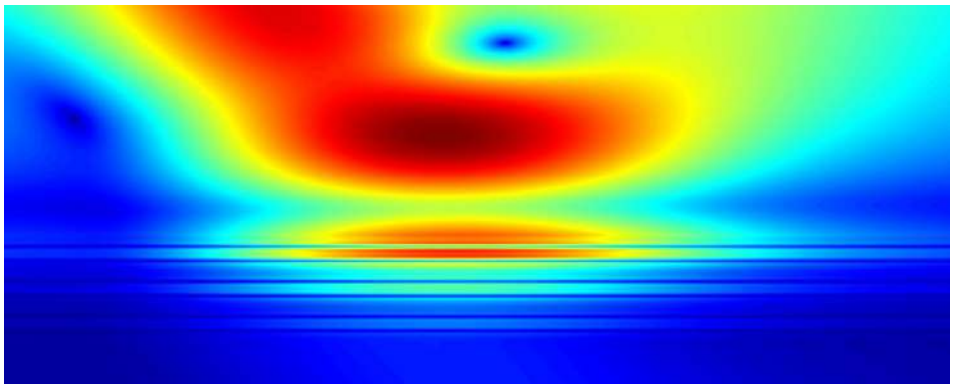


FIGURE 2.13: Negative refraction of a Gaussian beam with a waist of 50λ, propagating in air and meeting a hyperbolic meta material as described in [44]. The working wavelength is 363.8 nm, the incidence angle $75°$. The physical width of the domain is 15λ nm and the height 2000 nm. The picture has been stretched to be easier to understand.

This means that when the size of the gap decreases, since the effective index diverges, the size of the resonator decreases. In the work of Bozhevolnyi et al.[7], it has been explained that in thin strips and narrow gaps, both structures exhibit the same Q-factor of the resonance determined primarily by the complex dielectric function of metal. Moreover, the quality factor does not change when the size of the gap decreases. This increases the imaginary part of the propagation constant of the gap-plasmon, but the size of the resonator decreases too, so that finally the quality factor remains essentially constant. One of the consequences of such a miniaturization is that with so tiny cavities, the Purcell effect is huge in such structures. The Purcell factor measures the ratio between the lifetime of an emitter in vacuum to the lifetime in the cavity. A high Purcell factor thus means that the emitter can couple efficiently to its environment to emit light very quickly. Using MIM

resonators, a team from Duke University managed to reach up to 1000 for the Purcell factor[2].

Finally, it is worth mentioning that the miniaturization makes the optical resonators difficult to fabricate using lithography. But nanocubes can be synthesized and then auto-assembled on a metallic surface covered by a chemically grown spacer of a few nanometers, allowing to realize actual MIM resonators working in the visible range of the spectrum for a very low cost[29]. MIM resonators can be used for biosensing[9], and even nanocubes can be used for gas detection[38].

2.5.1 Dispersion relation

We will now look for the dispersion relation of the gap-plasmon, the even mode that propagates in a gap between two metals.

The form of the magnetic field H_y is in the upper metallic part

$$H_y = A\exp(\kappa_m z)\exp(ik_x x) \tag{2.64}$$

The form of the magnetic field H_y is in the lower metallic part

$$H_y = B\exp(-\kappa_m z)\exp(ik_x x) \tag{2.65}$$

In the dielectric the form of the magnetic field H_y is

$$H_y = [C\exp(\kappa_d z) + D\exp(-\kappa_d.z)]\exp(ik_x x) \tag{2.66}$$

The gap-plasmon being an even mode, $C = D$ and we have in the dielectric

$$H_y = E\cosh(\kappa_d z)\exp(ik_x x) \tag{2.67}$$

The boundary conditions, H_y and $\frac{1}{\varepsilon}\frac{\partial H_y}{\partial z}$ being continuous, lead for $z = \frac{h}{2}$ as shown in figure 2.14 to

$$E\cosh(\kappa_d\frac{h}{2}) = A\exp(-\kappa_m\frac{h}{2}) \tag{2.68}$$

and

$$E\sinh(\kappa_d\frac{h}{2}) = A\left[-\frac{\kappa_m}{\varepsilon_m}\exp(-\kappa_m\frac{h}{2})\right]. \tag{2.69}$$

Taking the ratio of the above equations yields the dispersion relation

$$\frac{\kappa_m}{\varepsilon_m} + \frac{\kappa_d}{\varepsilon_d}\tanh(\kappa_d\frac{h}{2}) = 0. \tag{2.70}$$

Here there is no way to explicitly write k_x as a function of ω. The solutions of the equation have to be computed in the complex plane, using Moosh. As can be easily seen however, when $h \to +\infty$ the dispersion relation is simply the dispersion relation of the surface plasmon as shown in figure 2.14. We have nonetheless tried to redo the calculations leading to analytic expressions for the group and energy velocity.

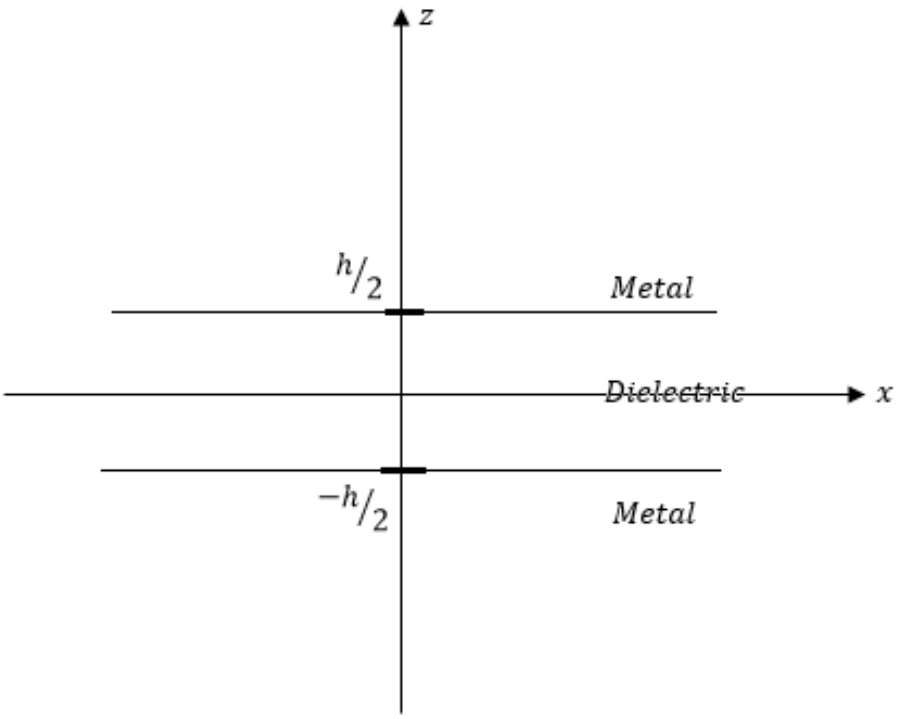


FIGURE 2.14: The waveguide in which the gap-plasmon propagates

2.5.2 Group velocity

We begin with the dispersion relation, that can be written

$$g(k_x, \omega) = \frac{\kappa_m}{\varepsilon_m} + \frac{\kappa_d}{\varepsilon_d} \tanh(\kappa_d \frac{h}{2}) = 0. \tag{2.71}$$

The dispersion relation is not as simple as for surface plasmons where k_x is an explicit function of ω. The group velocity can thus be calculated using the relation

$$v_g = -\frac{\frac{\partial g}{\partial k_x}}{\frac{\partial\, g}{\partial \omega}}. \tag{2.72}$$

We first calculate the term

$$\frac{\partial g}{k_x} = \frac{1}{\varepsilon_m} \frac{\kappa_m}{\partial k_x} + \frac{1}{\varepsilon_d} \frac{\kappa_d \tanh(\kappa_d \frac{h}{2})}{\partial k_x} \tag{2.73}$$

which gives

$$\frac{\partial g}{\partial k_x} = \frac{k_x[2\kappa_d \varepsilon_d + 2\kappa_m \varepsilon_m \tanh(\kappa_d \frac{h}{2}) - h\kappa_m \kappa_d]\text{sech}^2(\kappa_d \frac{h}{2})}{2\kappa_m \kappa_d \varepsilon_m \varepsilon_d} \tag{2.74}$$

and finally

$$\frac{\partial g}{\partial \omega} = \frac{1}{\varepsilon_m}\frac{\partial \kappa_m}{\partial \omega} + \frac{1}{\varepsilon_d}\frac{\partial \kappa_d \tanh(\kappa_d \frac{h}{2})}{\partial \omega}. \tag{2.75}$$

The second term can be written

$$\frac{\partial g}{\partial \omega} = -\frac{\omega[2\kappa_d + 2\kappa_m \tanh(\kappa_d \frac{h}{d}) + \kappa_m \kappa_d h\omega \,\mathrm{sech}^2(\kappa_d \frac{h}{2})]}{2\kappa_m \kappa_d c^2} \tag{2.76}$$

and thus the group velocity can be written under the form

$$v_g = \frac{[2\kappa_d + (2\kappa_m \varepsilon_m)\tanh(\kappa_d \frac{h}{2}) - (h\kappa_m \kappa_d \mathrm{sech}^2(\kappa_d \frac{h}{2}))[\varepsilon_m^2]\tanh^2(\kappa_d \frac{h}{2})]}{2\kappa_d + 2\kappa_m \tanh(\kappa_d \frac{h}{2}) + \kappa_m \kappa_d h \mathrm{sech}^2(\kappa_d \frac{h}{2})\,(\tanh^2(\kappa_d \frac{h}{2}\varepsilon_m^3 \varepsilon_d^2)} \tag{2.77}$$

2.5.3 Energy velocity

Again, the energy velocity is, in the non-dispersive case,

$$v_E = \frac{\int_{-\infty}^{+\infty} P dz}{\int_{-\infty}^{+\infty} \xi dz} \tag{2.78}$$

In order to calculate v_E, the following steps should be done

$$P_m^1 = \frac{k_x}{\omega \varepsilon_0 \varepsilon_m} \exp(2\kappa_m z) \tag{2.79}$$

$$P_m^2 = \frac{k_x}{\omega \varepsilon_0 \varepsilon_m} \exp(-2\kappa_m z) \tag{2.80}$$

$$P_d = \frac{k_x[\exp(2\kappa_d z) + \exp(-2\kappa_d z)] + 2}{\omega \varepsilon_0 \varepsilon_d} \tag{2.81}$$

$$\int_{-\infty}^{+\infty} P dz = \int_{-\infty}^{-\frac{h}{2}} P_m^1 dz + \int_{-\frac{h}{2}}^{\frac{h}{2}} P_d dz \int_{\frac{h}{2}}^{+\infty} P_m^2 dz \tag{2.82}$$

$$\int P_m dz = \frac{k_x \exp(-\kappa_m h)}{\kappa_m \varepsilon_0 \varepsilon_m \omega} \tag{2.83}$$

$$\int_{-\frac{h}{2}}^{+\frac{h}{2}} P_d dz = \frac{k_x[\exp(\kappa_d h) - \exp(-\kappa_d h) + 2\kappa_d h]}{\kappa_d \varepsilon_0 \varepsilon_d \omega}$$

$$\int_{-\infty}^{+\infty} P dz = \int P_m dz + \int P_d dz \tag{2.84}$$

$$\int P_m dz = \frac{k_x \exp(-\kappa_m h)}{\kappa_m \varepsilon_0 \varepsilon_m \omega} \tag{2.85}$$

$$\int P_d dz = \frac{k_x(\exp(\kappa_d h) - \exp(-\kappa_d h) + 2\kappa_d h)}{\kappa_d \varepsilon_0 \varepsilon_d \omega} \tag{2.86}$$

The calculations of the stored energy density are shown below

$$\xi_m^1 = \frac{\kappa_m \exp(2\kappa_m z)}{\varepsilon_0 \varepsilon_m \omega} \tag{2.87}$$

$$\xi_m^2 = \frac{\kappa_m \exp(-2\kappa_m z)}{\varepsilon_0 \varepsilon_m \omega} \tag{2.88}$$

$$\xi_d = \frac{\kappa_d [\exp(2\kappa_d z) + \exp(-2\kappa_d z)]}{\varepsilon_0 \varepsilon_d \omega} \tag{2.89}$$

Where ξ_m^1 and ξ_2^m are the stored energy densities in the two metallic slabs and ξ_d is the stored energy density in the dielectric. The total energy density is the sum of the energy densities in the two metallic slabs and the dielectric. And in order to calculate the energy velocity in a gap plasmon the total energy density should be integrated. This is shown in equation 2.94

$$\int_{-\infty}^{+\infty} \xi dz = \int_{-\infty}^{-\frac{h}{2}} \xi_m^1 dz + \int_{\frac{h}{2}}^{+\infty} \xi_m^2 dz + \int_{-\frac{h}{2}}^{\frac{h}{2}} \xi_d dz \tag{2.90}$$

$$\int \xi_m = \frac{1}{\varepsilon_0 \varepsilon_m} \exp(-\kappa_m h) \tag{2.91}$$

$$\int \xi_d dz = \frac{2 \sinh(\kappa_d h)}{\varepsilon_0 \varepsilon_d \omega} \tag{2.92}$$

$$\int_{-\infty}^{+\infty} \xi dz = \frac{\varepsilon_d \exp(-\kappa_m h) + 2\varepsilon_m \sinh(\kappa_d h))}{\varepsilon_0 \varepsilon_m \varepsilon_d \omega} \tag{2.93}$$

Then by applying equation 2.68, the energy velocity is calculated

$$v_E = \frac{k_x(\varepsilon_d \exp(-\kappa_m h) + 2\varepsilon_m(\sinh(\kappa_d h) + \kappa_d h))}{\kappa_m \kappa_d(\varepsilon_d \exp(-\kappa_m h) + 2\varepsilon_m \sinh(\kappa_d h))} \tag{2.94}$$

2.5.4 Prism coupler and gap-plasmons

Exciting a gap-plasmon can be both easy and difficult. For instance, it is hard to excite a gap-plasmon using a fire-end coupler. The width of the gap is so small that the incoming wave has difficulties to couple to the guided mode. Typically, when illuminating two coupled nanocubes, whereas there is a gap-plasmon resonance in between, it gives a very small signal.

There is however a way to excite gap-plasmon that has never been explored yet, although it is very simple. One can use a prism to couple a gap-plasmon. Of course, this way to excite the gap-plasmon is limited: the maximum effective index that can be reached is the index of the prism. The highest index prism is made of TiO_2 with an index of approximately 2.6. This means that when the gap is too narrow, the effective index of the gap-plasmon is so high that it cannot be excited any more.

The reflection coefficient of the structure (prism-metal-gap-metal) can be simulated, once more, using Moosh. The result show that the gap-plasmon

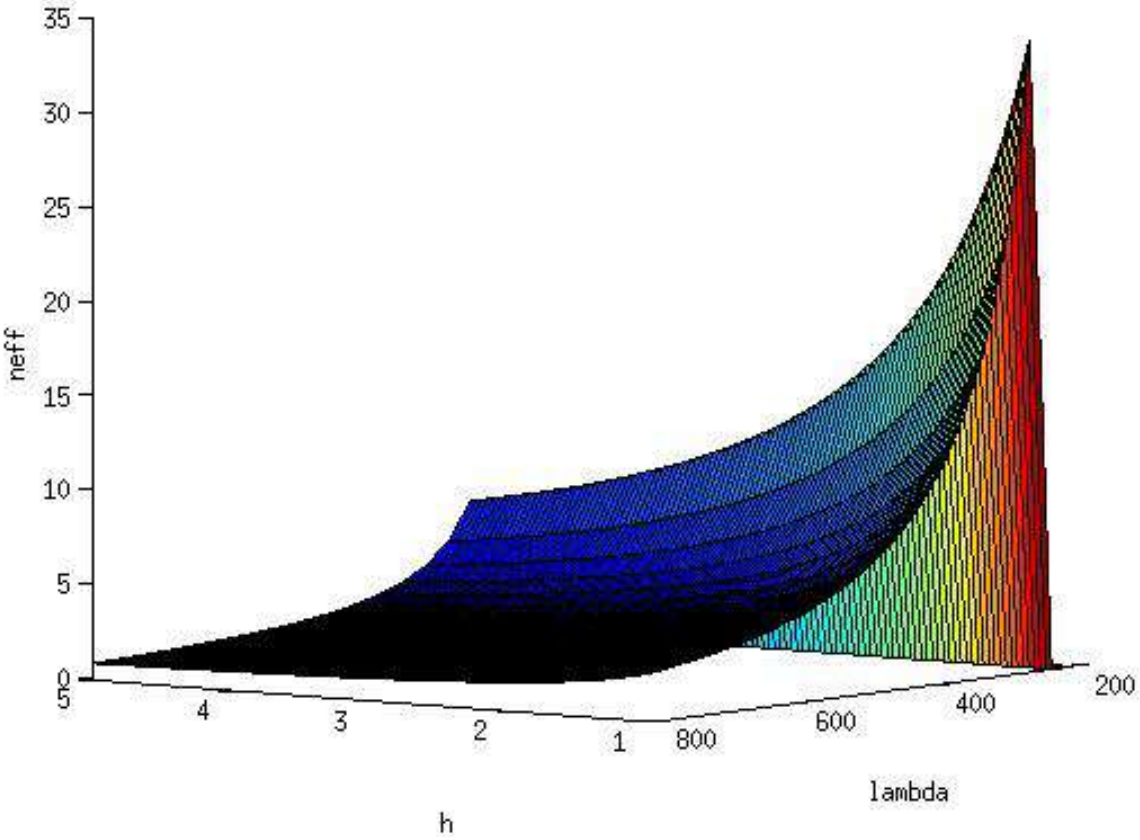


FIGURE 2.15: The effective index as a function of the plasmon frequency and the width of the gap

can actually be excited (see figure2.16). Of course, the excitation depends on the thickness of the gold layer, just like for the surface plasmon. The narrower the gap, the higher the effective index, and thus the larger the incidence angle for which the resonance is excited.

When the gap is narrower than 12 nanometers, obviously the gap-plasmon resonance is difficult to couple, as its effective index is too high. A gap in the reflection still persists, but it is much less pronounced and shifts slightly towards smaller angles.

Figure 2.17 shows the map of the magnetic field when a gap-plasmon resonance is excited, computed using Moosh.

2.6 Conclusion

In this chapter, we have shown the main conceptual "objects" on which the field of plasmonics relies. The most fundamental concept is the concept of surface plasmon: a mode that is guided along an interface between a metal

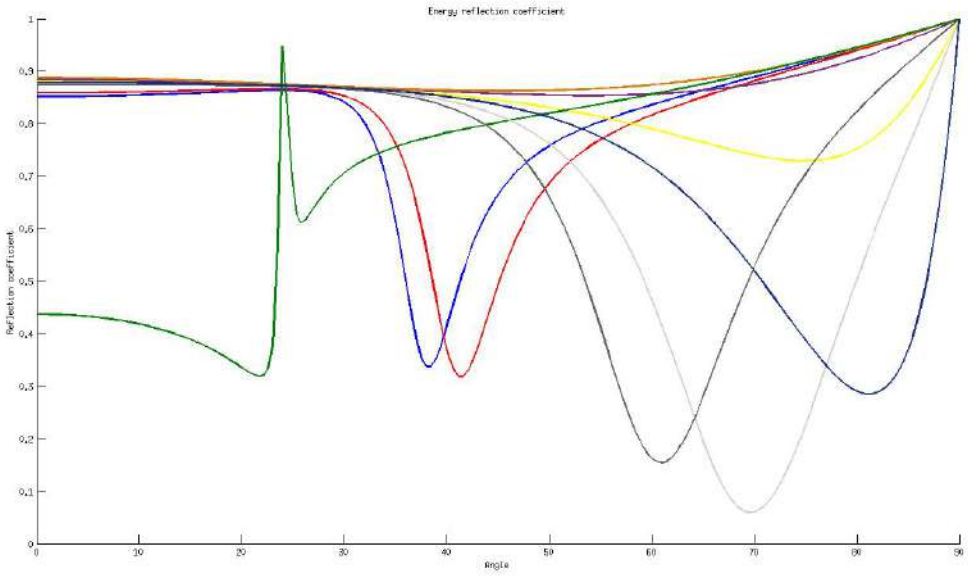


FIGURE 2.16: Gap Plasmon Resonance. Energy reflection coefficient as a function of the incident angle with a wavelength of 600 nm,spatial window size $d = 70\lambda$ and an incident beam width $w = 10\lambda$, the green curve represents a gap of width 1000nm and the rest are as follows: blue with gap of 50nm, the red curve represents: 20 nm gap, the dark gray curve represents the gap of 18nm width, the gray curve represents the gap of 15nm width, the dark blue curve represents the gap of 12nm width, the yellow curve with a gap of 10nm width, the purple curve represents the gap of 5nm width.

and a dielectric. This is still today the most important contribution of plasmonics to applied physics, as using prism couplers allowing for the excitation of surface plasmon resonance (SPR) is a widespread sensing method for biologically interesting molecules. We have tried to illustrate as much as possible, using Moosh, all the concepts of plasmonics. And we have calculated analytically the group velocities and energy velocities of the surface plasmon and of the gap-plasmon, the guided modes between two metals. This has shown that in non-dispersive cases, even in the presence of metal, Yariv and Yeh's theorem holds - so that there seems to be no need to take into account the electrons in the energetic point of view. This is a first result. We were not able however to tell from the expressions we have calculated in the dispersive case, what we should take as an expression for the local energy density. This will be discussed in the next chapter.

Recently, gap-plasmons, guided modes between two metals, with the remarkable property to present very high effective index when the gap is very small, have been studied and identified as the next important concept of plasmonics. The fact that they propagate so slowly is leveraged to built sub wavelength resonators. But the physics of this slowdown could benefit

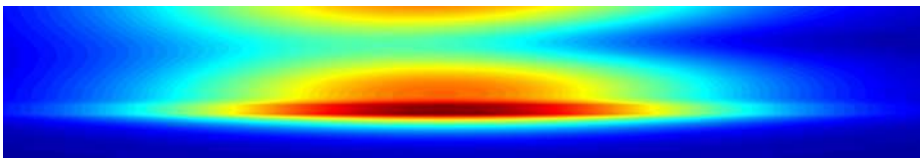


FIGURE 2.17: Gap Plasmon Resonance with a wavelength of 600 nm,spatial window size $d = 70\lambda$ and an incident beam width $w = 10\lambda$

from a new vision - as it is difficult to form any intuition about why exactly this plasmonic slowdown takes place. Anyway, we have shown that it is possible theoretically, using high index prisms, to excite the equivalent of the SPR for the gap-plasmon, the Gap-Plasmon Resonance. This will be useful in the last chapter, when non-local phenomena kick in.

Chapter 3

The Energy Point of View in Plasmonics: The Concept of Plasmonics Drag

Introduction

We have discussed in the previous chapter the properties of gap-plasmons, and their tendency to present a very high effective index when the width of the gap decreases - and how this explains the extraordinary small size of gap-plasmon resonators compared to the wavelength in vacuum. Even though the dispersion relation completely allows to describe this phenomenon, a more physical view of this phenomenon has yet to be provided. Gap-plasmons are characterized by effective wavelengths that can theoretically be as small as a tenth of the wavelength in vacuum, so that even very deeply sub wavelength structures can resonate. There is however little physical insight into the reasons why gap-plasmons do actually reach so small wavelengths and thus so large wave vectors.

In this chapter we show that considering how the energy flows in metals, gives a coherent physical picture of guided modes in plasmonics, and thus of the gap-plasmon behavior. We rely on the work of Yariv and Yeh, who showed that the velocity energy is equal to the group energy for modes guided in non-dispersive, dielectric multi-structures. We generalized their theorem to plasmonic guided modes, that propagate in metals, even though metals are intrinsically dispersive and contain electrons, making the right expression for the energy flux and density subject to debate. Then we use the insight brought by the theorem to study surface plasmons and gap-plasmons, showing the insight this approach can bring.

3.1 Energy velocity in metals

In non-dispersive, dielectric media, Poynting's theorem allows to give clear expressions for the Poynting vector $\vec{\Pi}$, representing the energy flux, and the energy density ξ. Building on these, it is possible to define, for a guided mode in a dielectric multilayer, the energy velocity. Defining the energy velocity is useless, unless it can be somehow linked to other velocities, to provide an insight on the way these modes propagate. Yariv and Yeh have

shown that for any mode guided in a dielectric structure, energy velocity and group velocity are actually equal. This theorem has limited importance, as the energy in dielectric structures is totally unable to flow in any exotic way.

Yariv and Yeh's result can not be applied directly to modes guided in plasmonic structures like multilayers for two reasons (i) the expression of the energy cannot be correct, as metals present a negative permittivity and because they are intrinsically dispersive, and even more importantly (ii) electrons, that are responsible for the optical response of metals, carry a large part of the energy so that the Poynting vector and the energy density in plasma have completely different expressions. But since plasmonic structures exhibit very exotic behaviors, as slow modes or negative refraction, considering the way the energy flows in these structures can be expected to provide much more insight than for dielectric waveguides.

In this first part we show, taking the same path as Yariv and Yeh, that considering the energy carried by the electromagnetic fields only is enough to define properly an energy velocity that is actually equal to the group velocity for guided modes in structures containing metals. This provides a justification for previous works where the Poynting vector has been show to actually provide some insight into the propagation of plasmonic guided modes and Bloch modes.

We underline that we establish this link in the framework of the Drude model, without taking into account the losses. In plasmonic structures, losses are usually important. Here, however, they will not hinder us from discussing important features of plasmonic structures as negative refraction and slow modes. It should however be kept in mind that when interband transition kick in, the losses become so high that modes simply do not propagate any more. We will probably never be able to witness the excitation of a plasmonic backward mode, although they have been theoretically predicted, because they are supported only for very high frequencies for which losses are overwhelming.

We consider a multilayered structure invariant in the x and y directions, and a guided mode, solution of Maxwell's equations presenting a $e^{i(k_x\,x-\omega\,t)}$ dependency in x and t. In the following, we call k_x/k_0 where $k_0 = \frac{\omega}{c}$ the effective index of the guided mode. We will assume the mode is p-polarized, because nothing exotic occurs for the s polarization in metallo-dielectric structures. Maxwell's equations reduce to

$$\begin{aligned} \partial_z E_z - ik_x E_z &= i\omega\mu_0 H_y && (3.1)\\ \partial_z H_y &= i\omega\epsilon_0\epsilon E_x && (3.2)\\ ik_x H_y &= -i\omega\epsilon_0\epsilon E_z && (3.3) \end{aligned}$$

Any change in the mode will be linked to a small change in its propagation constant, noted δk_x, its pulsation $\delta\omega$, its electric and magnetic field, respectively $\delta\vec{E}$ and $\delta\vec{H}$. These small changes are all linked by Maxwell's equations, whatever the dispersion relation. These equations can thus be

differentiated to yield

$$\begin{aligned} -i\,\delta k_x\,E_z - ik_x\,\delta E_z + \partial_z\,\delta E_x &= -i\,\delta\omega\,\mu_0 H_y - i\omega\mu_0\,\delta H_y && (3.4)\\ \partial_z\,\delta H_y &= i\,\delta\omega\,\epsilon_0\epsilon\,E_x + i\omega\epsilon_0\,\delta\epsilon\,E_x + i\omega\epsilon_0\epsilon\,\delta E_x && (3.5)\\ i\,\delta k_x\,H_y + ik_x\,\delta H_y &= -i\,\delta\omega\,\epsilon_0\epsilon E_z - i\omega\epsilon_0\,\delta\epsilon\,E_z - i\omega\epsilon_0\epsilon\,\delta E_z && (3.6)\end{aligned}$$

and since ϵ is only a function of ω, we can write that $\delta\epsilon = \delta\omega\,\frac{\partial\epsilon}{\partial\omega}$.

Following Yariv and Yeh, we introduce now the quantity

$$\vec{F} = \delta\vec{E}\otimes\vec{H}^* + \delta\vec{H}^*\otimes\vec{E} + \vec{H}\otimes\delta\vec{E}^* + \vec{E}^*\otimes\delta\vec{H}, \qquad (3.7)$$

where * denotes the complex conjugate.

Since we restrain ourselves here to a multilayered structure invariant in the y direction, we only need to calculate $\partial_z F_z = 2i\partial_z\Im\left(\delta E_x\,H_y^* - E_x\,\delta H_y^*\right)$. Given this expression, we first calculate the quantity

$$\begin{aligned}\mathbb{A} &= \partial_z\left(\delta E_x\,H_y^* - E_x\,\delta H_y^*\right)\\ &= \partial_z\delta E_z.H_y^* + \delta E_x.\partial_z H_y^* - \partial_z\,\delta H_y^*.E_x + \delta H_y^*.\partial_z E_x\end{aligned}$$

Using respectively (3.4),(3.5) and (3.6) we find that the different terms can be written

$$\begin{aligned}\partial_z(\delta E_x)H_y^* &= i\,\delta k_x\,E_z H_y^* + ik_x H_y^*\,\delta E_z + i\,\delta\omega\,\mu_0|H_y|^2 + i\omega\mu_0\,\delta H_y\,H_y^* && (3.8)\\ \partial_z H_y^*.\delta E_x &= -i\omega\epsilon\epsilon E_x^*\,\delta E_x && (3.9)\\ -\partial_z(\delta H_y^*)E_x &= i\,\delta\omega\,\epsilon_0\left(\epsilon + \omega\,\frac{\partial\epsilon}{\partial\omega}\right)|E_x|^2 + i\omega\epsilon_0\epsilon\,\delta E_x^*\,E_x && (3.10)\\ -\delta H_y^*\,\partial_z E_x &= -ik_x E_z\,\delta H_y^* + i\omega\mu_0 H_y\,\delta H_y^* && (3.11)\end{aligned}$$

Using (3.3) and (3.6), we have in addition

$$ik_x\left(\delta E_z H_y^* - E_z\,\delta H_y^*\right) = -\delta E_z\,i\omega\epsilon_0\epsilon E_z^* + i\omega\epsilon_0\epsilon\,\delta E_z^*\,E_z + i\delta k_x\,E_z H_y^* + i\delta\omega\epsilon_0\left(\epsilon + \omega\,\frac{\partial\epsilon}{\partial\omega}\right)|E_z|^2. \qquad (3.12)$$

Adding all the terms to calculate A and using (3.12), we finally get

$$\partial_z F_z = 4i\,\delta k_x\Re\left(E_z H_y^*\right) + 2i\,\delta\omega\left(\mu_0|\vec{H}|^2 + \epsilon_0\left\{\epsilon + \omega\,\frac{\partial\epsilon}{\partial\omega}\right\}|\vec{E}|^2\right) \qquad (3.13)$$

where all the real terms have been eliminated. We recognize the expression of the Poynting vector and an expression that we identify as the energy density in a dispersive medium $\xi = \frac{1}{4}\left(\mu_0 H_y H_y^* + \left\{\epsilon + \omega\,\frac{\partial\epsilon}{\partial\omega}\right\}\vec{E}.\vec{E}^*\right)$.

When $\partial_z F_z$ is integrated over the whole profile of a guided mode in a plasmonic structure, we thus get

$$\int_{-\infty}^{+\infty} \partial_z F_z = 0 \tag{3.14}$$

$$= -8i\delta k_x \int \Pi_x \mathrm{d}z + 8i\delta\omega \int \xi \mathrm{d}z \tag{3.15}$$

so that finally we have the theorem

$$v_E = \frac{\int \pi_x dz}{\int \xi dz} = \frac{\partial \omega}{\partial k_x} = v_g \tag{3.16}$$

Our conclusion is that, for a plasmonic guided mode propagating partially inside metals, the theorem of Yariv and Yeh holds. This means that considering the energy flow of the electromagnetic guided mode solely is sufficient to get a sense of what really happens to the energy and to be able to do a link with the group velocity. There may be a component of the energy density and energy flow that come from the free electrons, and it could be worth to go and explore this peculiar point. But obviously, considering an energy density taking into account dispersion but not the electrons movement is enough.

Most importantly, this means that considering the guided modes by looking at the Poynting flow makes perfect sense. This is crucial because energy flows strangely enough in metals - in a way opposite to the propagation direction given by the wavevector. This alone, as we will show in the following, gives and explanation about the low group velocity and high effective index of plasmonic guided modes.

Finally, it is worth underlining that this demonstration provides a way to reach an expression for the energy density for dispersive materials that is completely different from the many ways to do so proposed by Brillouin, Landau or Loudon[32].

3.2 Energy flow for surface plasmons

Our aim here is to consider the surface plasmon through the prism of energy and to make energy balances. We first underline that, in the framework of Drude's model, we can write that

$$\varepsilon + \omega \frac{\partial \varepsilon}{\partial \omega} = 1 - \frac{\omega_p^2}{\omega^2} + \omega \left[\frac{2\omega_p^2}{\omega^3} \right] = 1 + \frac{\omega_p^2}{\omega^2} \tag{3.17}$$

3.2.1 Energy velocity

We will here calculate the energy density using the right expression for the energy of the electromagnetic wave only. Again, while the calculations can

prove tiresome and are really complicated by the fact that the metal is dispersive, the expressions they give for the energy (and thus group) velocity have the advantage of being easy to discuss because at the numerator the Poynting balance appears.

If we take, again, for the magnetic field in the dielectric $H_y = A\exp(-i\kappa_d z)$ we have

$$E_x = \frac{-A\kappa_d \exp(-\kappa_d z)}{j\omega\varepsilon\varepsilon_d} \tag{3.18}$$

and

$$E_z = \frac{Ak_x \exp(-\kappa_d z)}{\omega\varepsilon_0\varepsilon_d} \tag{3.19}$$

while inside the metal the expressions for the fields are

$$H_y = A\exp(\kappa_m z) \tag{3.20}$$

and again for the electric fields inside the metal

$$E_x = \frac{A\kappa_m \exp(\kappa_m z)}{i\omega\varepsilon_0\varepsilon_m} \tag{3.21}$$

$$E_z = \frac{Ak_x \exp(\kappa_m z)}{i\omega\varepsilon_0\varepsilon_m} \tag{3.22}$$

The energy density is

$$\xi = \frac{1}{4}\mu_0 H_y H_y^* + \varepsilon_0\left(\varepsilon + \omega\frac{\partial\varepsilon}{\partial\omega}\right)[E_x E_x^* + E_z E_z^*] \tag{3.23}$$

In the dielectrics, the energy density is

$$\xi_d = \frac{1}{4}\mu_0|A|^2\exp(-2\kappa_d z) + \frac{1}{4}\frac{\varepsilon_0\varepsilon_d[\kappa_d^2 + k_x^2]}{\omega^2\varepsilon_0^2\varepsilon_d^2}|A|^2\exp(-2\kappa_d z) \tag{3.24}$$

Since $k_d^2 = k_x^2 - \varepsilon_d k_0^2$, we have

$$\xi_d = \frac{1}{4}\mu_0|A|^2\exp(-2\kappa_d z)\left[1 + \frac{1}{\omega^2\mu_0\varepsilon_0\varepsilon_d}[2k_x^2 - \varepsilon_d k_0^2]\right]. \tag{3.25}$$

Since $k_0^2 = \omega^2\mu_0\varepsilon_0$, then

$$\xi_d = \frac{1}{4}|A|^2\exp(-2\kappa_d z)\frac{2k_x^2}{\varepsilon_d\omega\varepsilon_0} \tag{3.26}$$

and

$$\int_0^{+\infty}\xi_d dz = \frac{k_x^2}{4\omega^2\varepsilon_0\varepsilon_d\kappa_d}|A|^2. \tag{3.27}$$

In the metal and since,$\kappa_m^2 = k_x^2 - \varepsilon_m k_0^2$, the energy density is

$$\xi_m = \frac{1}{4}\mu_0|A|^2\exp(2\kappa_m z) + \frac{1}{4}\varepsilon_0\left(1+\frac{\omega_p^2}{\omega^2}\right)\frac{1}{\omega^2\varepsilon_0^2\varepsilon_m^2}\left[\kappa_m^2+k_x^2\right]|A|^2\exp(2\kappa_m z) \quad (3.28)$$

$$= \frac{1}{4}|A|^2\exp(2\kappa_m z)\left[\mu_0 + \frac{(1+\frac{\omega_p^2}{\omega^2})}{(\omega^2\varepsilon_0\varepsilon_m^2)}(2k_x^2-\varepsilon_m k_0^2)\right] \quad (3.29)$$

$$= \frac{1}{4}|A|^2\exp(2\kappa_m z)\left[\mu_0\left(1-\frac{1+\frac{\omega_p^2}{\omega^2}}{1-\frac{\omega_p^2}{\omega^2}}\right)+\frac{2k_x^2}{\omega^2\varepsilon_0\varepsilon_m^2}\left(1+\frac{\omega_p^2}{\omega^2}\right)\right], \quad (3.30)$$

while, the integral of the energy density in the metal is given by

$$\int_{-\infty}^{0}\xi_m dz = \frac{1}{8\kappa_m}\left[\mu_0\frac{2}{1-\frac{\omega^2}{\omega_p^2}}+\frac{2\mu_0 k_x^2}{k_0^2\varepsilon_m^2}\left(1+\frac{\omega_p^2}{\omega^2}\right)\right]. \quad (3.31)$$

3.2.2 Poynting flux

The Poynting flux is

$$P_x = \frac{k_x}{\omega\varepsilon_0\varepsilon}|H_y|^2 \quad (3.32)$$

in the metal

$$\pi_m = \int_{-\infty}^{0}P_x dz = \frac{k_x}{2\omega\varepsilon_0\varepsilon_m\kappa_m}|A|^2 \quad (3.33)$$

and in the dielectric

$$\pi_d = \int_{0}^{+\infty}P_x dz = \frac{k_x}{2\omega\varepsilon_0\varepsilon_d\kappa_d}|A|^2 \quad (3.34)$$

$$\int P_x = \frac{k_x}{2\omega\varepsilon}\left[\frac{1}{\varepsilon_d\kappa_d}+\frac{1}{\varepsilon_m\kappa_m}\right] \quad (3.35)$$

The ratio of the flux is given by the simple expression

$$\frac{\pi_m}{\pi_d} = \frac{\kappa_d\varepsilon_d}{\kappa_m\varepsilon_m} \quad (3.36)$$

we have plotted this ratio as a function of the effective index on figure 3.1. It can be seen that, as the frequency approaches the surface plasmon frequency and thus the effective index tends to infinity, the ratio becomes important. This is the sign that high wavevector are directly linked to a ratio of the poynting in metal and in dielectric that become close to -1 (since the flux is negative in the metal). Such a ratio can be interpreted as a drag - the mode being violently slowed down by the negative Poynting vector of the metal.

3.3 Energy balance for gap-plasmons

For gap-plasmons too, the same kind of calculation can be made.

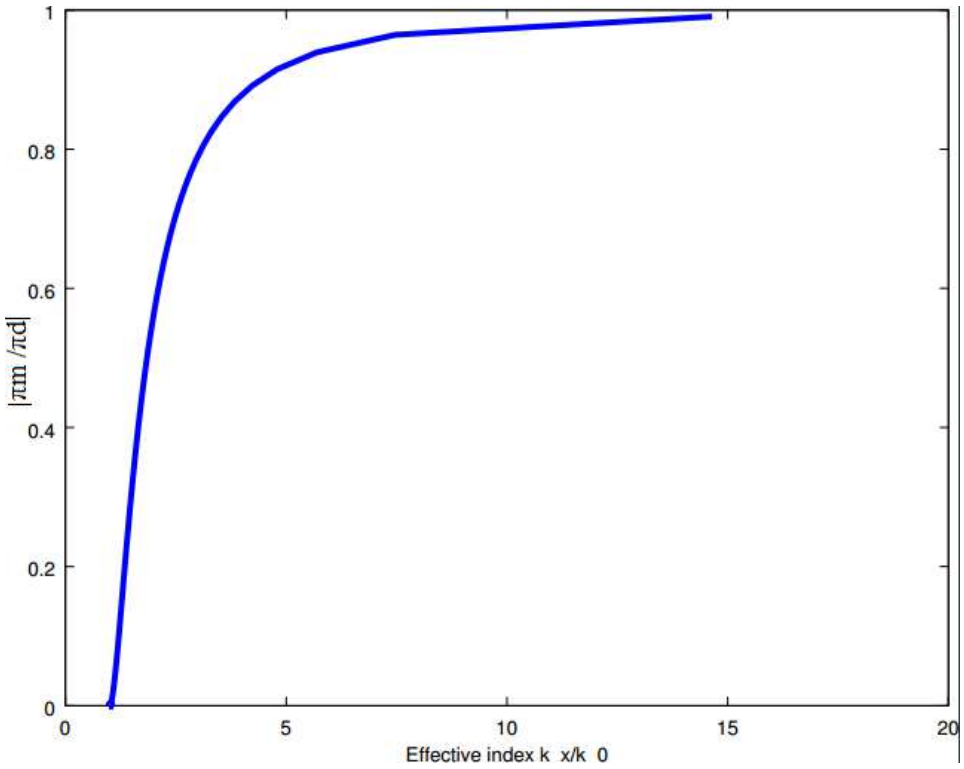


FIGURE 3.1: Ratio of the Poynting in metal (negative) to the Poynting in the dielectric for various effective index.

First we remind the reader the expressions of the fields (for $z > 0$, H_y and E_x being even and E_x odd with respect to $z = 0$):

$$H_y = \begin{cases} A\cosh(\kappa_d z) & z < \dfrac{h}{2} \\ B\exp(-\kappa_m z) & z > \dfrac{h}{2} \end{cases} \tag{3.37}$$

$$E_x = \begin{cases} A\kappa_d \sinh(\kappa_d z)\dfrac{1}{i\omega\varepsilon_0\varepsilon_d} \\ -B\kappa_m \exp(-\kappa_m z)\dfrac{1}{i\omega\varepsilon_0\varepsilon_m} \end{cases} \tag{3.38}$$

$$E_z = \begin{cases} \dfrac{-k_x}{\omega\varepsilon_0\varepsilon_d} A\cosh(\kappa_d z) \\ \dfrac{-k_x}{\omega\varepsilon_0\varepsilon_m} B\exp(-\kappa_m z) \end{cases} \tag{3.39}$$

3.3.1 Poynting flux

The Poynting flux in the dielectric can be written

$$\int_0^{\frac{h}{2}} P_d dz = \int_0^{\frac{h}{2}} |A|^2 \frac{k_x}{2\omega\varepsilon_0\varepsilon_d} \cosh^2(\kappa_d z) dz \tag{3.40}$$

and since $\cosh^2 x = 1 + \cosh(2x)$ a way to write this term is

$$\int_0^{\frac{h}{2}} P_d dz = \frac{|A|^2}{2\omega\varepsilon_0\varepsilon_d} k_x \int_0^{\frac{h}{2}} 1 + \cosh(2\kappa_d z) dz \tag{3.41}$$

$$= \frac{|A|^2 k_x}{2\omega\varepsilon_0\varepsilon_d} \left[\frac{h}{2} + \frac{1}{2\kappa_d}\sinh(\kappa_d h)\right]. \tag{3.42}$$

In the metal, we have

$$\int_{\frac{h}{2}}^{+\infty} \frac{|B|^2}{2\omega\varepsilon_0\varepsilon_m} k_x \exp(-2\kappa_m z) = \frac{|B|^2}{4\omega\varepsilon_0\varepsilon_m\kappa_m} k_x \exp(-\kappa_m h) \tag{3.43}$$

and if we take $A = 1$ (an arbitrary choice for a guided mode), we end up having

$$\int_0^{+\infty} \pi_x dz = \frac{k_x}{2\omega\varepsilon_0}\left[\frac{h}{2\varepsilon_d} + \frac{1}{2\kappa_d\varepsilon_d}\sinh(\kappa_d h) + \cosh^2(\kappa_d\frac{h}{2})\frac{1}{2\varepsilon_m\kappa_m}\right]. \tag{3.44}$$

These expressions can be used to compute the ratio of the Poynting flux in the metal over the Poynting flux in the dielectric as a function of the gap width and frequency, as shown on figure 3.2 - which will be discussed below.

3.3.2 Integrated energy density

Energy density

- Non-dispersive case

In the metal

$$\xi_m = \frac{1}{4}\left(\mu_0 H_y H_y^* + \varepsilon_0\varepsilon\vec{E}\vec{E}^*\right) \tag{3.45}$$

$$= \frac{1}{4}\mu_0|B|^2\exp(-2\kappa_m z) + \varepsilon_0\varepsilon_m|B|^2\frac{\kappa_m^2 + k_x^2}{4\omega^2\varepsilon_0^2\varepsilon_m^2}\exp(-2\kappa_m z) \tag{3.46}$$

$$= \frac{|B|^2 k_x^2}{4\omega^2\varepsilon_0\varepsilon_m}\exp(-2\kappa_m z) \tag{3.47}$$

$$\int_{\frac{h}{2}}^{+\infty} \xi_m dz = \frac{k_x^2}{4\omega^2\varepsilon_0\varepsilon_m\kappa_m}|B|^2\exp(-\kappa_m h) \tag{3.48}$$

In the dielectric

$$\xi_d = \frac{1}{4}\mu_0|A|^2\cosh^2(\frac{\kappa_d z}{2}) + \frac{1}{4}\varepsilon_0\varepsilon_d\left(\frac{1}{(\omega\varepsilon_0\varepsilon_d)^2}|A|^2\kappa_d^2\sinh^2(\kappa_d z) + \frac{k_x^2}{\omega^2\varepsilon_0^2\varepsilon_d^2}|A|^2\cosh^2(\frac{\kappa_d z}{2})\right) \tag{3.49}$$

The integral of energy density in the dielectric is done as follows

$$\int_0^{\frac{h}{2}} \xi_d dz = |A|^2 \left[\frac{1}{4}\mu_0 + \frac{k_x^2}{4\omega^2\varepsilon_0\varepsilon_d}\right] \int_0^{\frac{h}{2}} \cosh^2(\kappa_d z)dz + |A|^2 \frac{\kappa_d^2}{4\omega^2\varepsilon_0\varepsilon_d} \int_0^{\frac{h}{2}} \sinh^2(\kappa_d z)dz \tag{3.50}$$

In order to perform the calculation, we use

$$\cosh^2(\kappa_d z) = \frac{1}{2}\left[\cosh(2\kappa_d z) + 1\right]$$

and

$$\begin{aligned} \int_0^{\frac{h}{2}} \cosh^2(\kappa_d z)dz &= \frac{1}{2}\left[\frac{\sinh(2\kappa_d z)}{2\kappa_d} + z\right] && (3.51)\\ &= \frac{h}{4} + \frac{1}{4\kappa_d}\sinh(\kappa_d h). && (3.52) \end{aligned}$$

and

$$\begin{aligned} \int_0^{\frac{h}{2}} \sinh^2(\kappa_d z)dz &= \frac{1}{2}\left[\frac{\cosh(2\kappa_d z)}{2\kappa_d} - z\right] && (3.53)\\ &= \frac{-h}{4} + \frac{1}{4\kappa_d}\cosh(\kappa_d h). && (3.54) \end{aligned}$$

then the integral of the energy density in the dielectric is

$$\begin{aligned} \int_0^{\frac{h}{2}} \xi_d dz &= |A|^2 \left[\frac{1}{4}\mu_0 + \frac{k_x^2}{4\omega^2\varepsilon_0\varepsilon_d}\right]\left[\frac{h}{4} + \frac{1}{4\kappa_d}\sinh(\kappa_d h)\right] && (3.55)\\ &= \frac{h}{4} + \frac{1}{4\kappa_d}\sinh(\kappa_d h). && (3.56) \end{aligned}$$

$$\int_0^{\frac{h}{2}} \xi_d dz = |A|^2 \left[\frac{1}{4}\mu_0 + \frac{k_x^2}{4\omega^2\varepsilon_0\varepsilon_d}\right]\left[\frac{h}{4} + \frac{1}{4\kappa_d}\sinh(\kappa_d h)\right] + |A|^2 \frac{\kappa_d^2}{4\omega^2\varepsilon_0\varepsilon_d}\left[\frac{-h}{4} + \frac{1}{4\kappa_d}\cosh(\kappa_d h)\right] \tag{3.57}$$

- Dispersive case

ξ_d does not change, but ξ_m does and it is shown below

$$\begin{aligned} \xi_m &= \frac{1}{4}|B|^2\exp(-2\kappa_m z) + \frac{1}{4}\varepsilon_0\left(1 + \frac{\omega_p^2}{\omega^2}\right)|B|^2\frac{\kappa_m^2 + k_x^2}{\omega^2\varepsilon_0^2\varepsilon_m^2}\exp(-2\kappa_m z) && (3.58)\\ &= \frac{1}{4}\mu_0|B|^2\exp(-2\kappa_m z)\left(1 - \frac{1+\frac{\omega_p^2}{\omega^2}}{1-\frac{\omega_p^2}{\omega^2}}\right) + \frac{k_x^2}{2\omega^2\varepsilon_0\varepsilon_m^2}|B|^2\exp(-2\kappa_m z)(1 + \frac{\omega_p^2}{\omega^2}) && (3.59) \end{aligned}$$

$$\int_0^{\frac{h}{2}} \xi_m = \left[\frac{1}{4}\mu_0 \left(\frac{-\frac{2\omega_p^2}{\omega^2}}{1-\frac{\omega_p^2}{\omega^2}} \right) + \frac{k_x^2}{2\omega^2\varepsilon_0\varepsilon_m^2} \right] |B|^2(\exp(-\kappa_m h) - 1) \tag{3.60}$$

3.3.3 Energy velocity

The energy velocity is

$$v_E = \frac{\int \pi_x dz}{\int \xi dz} \tag{3.61}$$

We have checked numerically that the group velocity corresponded to this complicated expression. Moreover, we have, as for the surface plasmon, represented on figure 3.2 the ratio of the Poynting in the metal and in the dielectric. The same phenomenon appears, of course : the ratio tends to -1 (and to 1 in absolute value) whenever the mode is slowed down, either because the gap closes or because the frequency approaches the surface plasmon frequency.

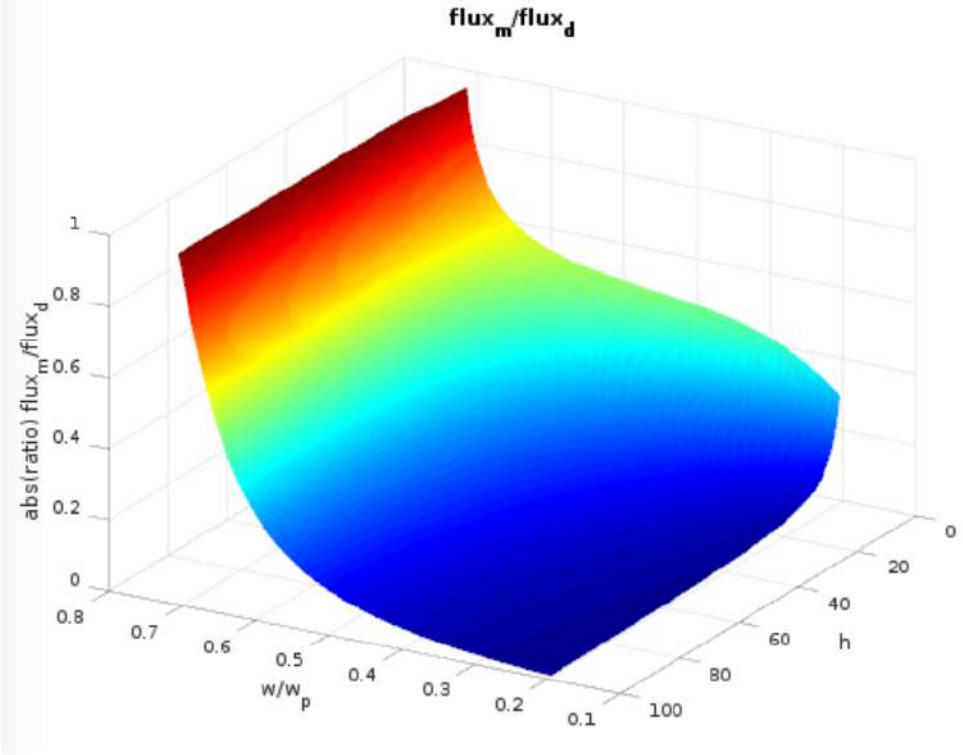


FIGURE 3.2: Ratio of the Poynting in metal (negative) to the Poynting in the dielectric as a function of the gap and of the frequency.

3.4 Conclusion

In this chapter, we have generalized Yariv and Yeh's theorem. Beyond this generalization, this means we have shown that considering the classical expression for the energy density in a dispersive medium was enough to be able to calculate an energy velocity of the electromagnetic field alone, and that this velocity is actually equal to the group velocity. There is thus no real need to consider the contribution of free electrons to the energy of the mode to discuss its physics. We underline that our work constitutes a way to reach an expression for the energy density different from all the previous, historical approaches by Brillouin or Landau.

We have shown on the examples of the surface plasmon and of the gap-plasmon that considering Poynting vector balances gives an completely new insight on why in plasmonic structures guided mode get slowed down. This energy point of view can be summarized by saying that the Poynting vector in metals is opposite to the propagation direction, so that metals produce a drag that diminishes the group velocity and thus increases the wavevector.

We finally stress that while we applied here our tools to guided modes, it is possible to reach the same conclusions for Bloch waves in metallo-dielectric structures - a study that remains to be done but that should be made easy by the theoretical developments we have presented here.

Chapter 4

Beyond Drude's Model: Non-locality in Plasmonics

Introduction

The Drude model is both extraordinary old and successful. Over the years, this incredible simple picture of electrons moving freely in the incoming electromagnetic field has allowed to describe the optical response of metal even for the smallest nanoparticles. There has been a huge amount of work dedicated to more accurate models of the jellium, the free electron gas contained in metals. The Thomas-Fermi model, for instance, has allowed historically to better understand the impressive accuracy of Drude's model[13]. Nowadays, we know the Drude model can be derived from the most fundamental laws of quantum mechanics - it represents the zero-th order term of any such model.

The hydrodynamic model has been developed and studied during the seventies and eighties. It constitutes a quite accurate framework to describe the non-linear response of metals. If the zero-th order is actually Drude's model, and the second-order terms are non-linear, there is a first order term which produces spatial dispersion. It it then no longer possible to describe the metal as a local dielectric - the polarization of the equivalent dielectric does not depend on the local electric field any more.

The influence of non-locality has been searched for years on surface plasmons and on nanoparticles. But surface plasmons never reach very high wavevectors and very small nanoparticles do not have a well controlled shape. All the theoretical developments that took place in the eighties did not produce any idea of any potential experiment showing nonlocal effects.

In 2012, such an experiment was published in Science[11]. Using a nanosphere coupled to a metallic film by a nanometric gap, Duke's team was able to show (at last) a difference between Drude's model predictions and the experiment. Moreover, they proved that the hydrodynamic model was very accurate and allowed to predict the right resonance shift when the particle was getting closer to the metallic substrate.

The main advantage of the hydrodynamic model is that is yields analytic results in multilayered structures. A paper was then published showing that gap-plasmons were much more likely to be sensitive to spatial dispersion

than any other plasmonic guided mode[28] because they could reach effective wavelength that are so small (not so far from the mean free path of electrons in metals). Finally, it is possible to write a scattering matrix method to solve Maxwell's equations in the framework of the hydrodynamic model[6], so that this feature has been included in Moosh[12].

I have used these tools to study the influence of nonlocality on the gap-plasmon resonance in the case of a prism coupler.

4.1 Local and nonlocal polarizability

Several models have been implemented in order to study the effect of the behavior of electrons on the electrical and optical properties of metallic structures. In all cases, the crucial quantity to estimate is the polarizability because, as has been shown in Chapter 2, any current of free electrons can be seen as an effective polarizability. Even in the case of the hydrodynamic model, this strategy holds.

4.1.1 Polarizability in Drude's model

The first model was the Drude model that was initiated around 1900. Considered to be the most accurate model for years, Drude's model clearly describe the movement of electrons in metals submitted to an external field. The most important characteristic of a metal, evidently, is its high electrical conductivity. So, around 1900, and shortly after J.J Thompson's discovered the electron, people became interested in the mechanism of metallic conduction - and no model had ever been proposed at the time. The earliest work had been performed by E. Riecke in 1898, but it was quickly invalidated by that of Drude in 1900[14]. Drude suggested a simple model that explained a notable empirical law, the Wiedermann Franz law[10] (1853). This law stated that at a given temperature the ratio of the thermal conductivity to the electrical conductivity was the same for all metals.

The assumptions of the Drude model are:

1. a metal contains free electrons which form an electron gas,
2. *there is now interaction between electrons, which interact only with the ionic crystal*
3. the average thermal energy of electrons is $<\frac{1}{2}mv_T^2>$. But, electrons pursue random movements inside the metal so that $<v_T>=0$ even though $<v_T^2> \neq 0$ (these random movements inside the metal are a result of collisions that occur with ions),
4. ions have large mass compared to electrons and thus they are essentially static.

In fact, the interaction between metals and electromagnetic radiation is mostly controlled by the conduction of electrons inside the metal and referring to

Drude Model, free electrons vibrate 180 degrees out of phase relative to the driving electric field[31]. As a result, all metals maintain a negative dielectric constant below their plasma frequency, which causes the very high reflectivity.

Considering the effects of free electrons, application of the Drude-Sommerfeld model for free electron-gas simply gives

$$m_e \frac{\partial^2 \vec{r}}{\partial t^2} + m_e \Gamma \frac{\partial \vec{r}}{\partial t} = e\vec{E}_0 \exp(-i\omega t) \tag{4.1}$$

where e and m_e are the charge and the effective mass of the free electrons, which is quite close to their actual mass for metals. $\vec{E}_0$ and ω are the complex amplitude and the frequency of the applied electric field. Γ is the damping term and is proportional to the Fermi velocity denoted by v_F and inversely proportional to the electron mean free path l between scattering events, $\Gamma = \frac{v_F}{l}$. The frequency-dependent dielectric function of the metal is given by

$$\varepsilon(\omega) = 1 + \chi_e(\omega) \tag{4.2}$$

and finally

$$\varepsilon_{Drude}(\omega) = 1 - \frac{\omega_p^2}{\omega^2 + i\Gamma\omega} \tag{4.3}$$

where $\omega_p = \sqrt{\frac{ne^2}{m_e \varepsilon_0}}$ is the plasma frequency.

It is possible to add terms representing the contribution of core electrons, the polarizability of the ionic crystal. This is especially important when studying spatial dispersion, as the response of free electrons is much more nonlocal than the response of the bound electrons.

In order to be as realistic as possible on this particular issue, we use fits made on a very large wavelength rang, based on many different experimental data[39]. They allow to distinguish between the two responses. The model used for the supplementary terms in this case is more complicated than the classical

4.1.2 Polarizability in the hydrodynamic model framework

As previously stated, the hydrodynamic model studies the collective motion of free electrons in metals, seen as a fluid. This motion is described in terms of hydrodynamic variables that are

- the charge density $n(\vec{r}, t)$,
- the electron fluid velocity: $v(\vec{r}, t)$,
- the pressure inside the jellium $p(\vec{r}, t)$,
- and the macroscopic electric and magnetic fields respectively denoted by: $\vec{E}(\vec{r}, t)$ and $\vec{B}(\vec{r}, t)$.

The equation of motion of the electric fluid is written as

$$n\frac{\partial \vec{v}}{\partial t} + n(\vec{v}.\partial\vec{\nabla})\vec{v} + \gamma n\vec{v} = -\frac{ne}{m_e}(\vec{E} + \vec{v} \times \vec{B}) - \frac{\vec{\nabla}p}{m_e} \tag{4.4}$$

where, again, γ is the phenomenological parameter taking into consideration the electron-ion collisions.

The current density is

$$\vec{J} = -en\vec{v} \tag{4.5}$$

Considering the equation of continuity

$$\dot{n} = \frac{1}{e}\vec{\nabla}.\vec{J} \tag{4.6}$$

and substituting the current density in its value in equation (4.4) gives

$$\frac{\partial \vec{J}}{\partial t} - \frac{\vec{J}}{en}\vec{\nabla}.\vec{J} - \vec{J}.\vec{\nabla}(\frac{\vec{J}}{en}) - \gamma\vec{J} = \frac{ne^2}{m_e}E - \frac{e}{m_e}\vec{J} \times B + e\frac{\vec{\nabla}p}{m_e} \tag{4.7}$$

Here we linearize the equation by neglecting higher-order terms and then substitute the electric polarization vector $\ddot{\vec{P}} = \vec{J}$. This expression links local polarization in the studied medium with the external electric field and the pressure:

$$\ddot{\vec{P}} + \gamma\dot{\vec{P}} = \frac{ne^2}{m_e}E + \frac{e}{m_e}\vec{\nabla}p. \tag{4.8}$$

The last element missing is a relation between the pressure and the electronic density n. This relationship has been evaluated by in the framework of the Thomas-Fermi model which gives the form of the electron quantum pressure to be

$$p(r,t) = \xi n(r,t)^{5/3} \tag{4.9}$$

where $\xi = (3\pi^2)^{2/3}\ h^2/(5m_e)$. The continuity equation, can be integrated in order to relate the electron density to the medium polarization to yield

$$n(r,t) = n_0 + \frac{1}{e}\vec{\nabla}.\vec{P}(r,t). \tag{4.10}$$

The term n_0 is the equilibrium charge density. We can then relate the gradient of p to the electron density n by

$$\frac{e}{m_e}\vec{\nabla}p = \frac{5}{3}\frac{e}{m_e}\xi n^{2/3}\vec{\nabla}n \tag{4.11}$$

and using the integrated expression (4.10) for n yields

$$\frac{e}{m_e}\vec{\nabla}p = \frac{5}{3}\frac{n_0^{2/3}}{m_e}\xi\vec{\nabla}(\vec{\nabla}.\vec{P}), \tag{4.12}$$

so that we obtain finally the equation relating the effective polarization of the metal to the external electric field:

$$-\beta^2\vec{\nabla}(\vec{\nabla}.\vec{P}) + \ddot{\vec{P}} + \gamma\dot{\vec{P}} = \varepsilon_0\omega_p^2\vec{E} \tag{4.13}$$

where ω_p= $\sqrt{\frac{ne^2}{\varepsilon_0 m_e}}$ is the plasmon frequency and β = $\sqrt{\frac{5}{3}\frac{n_0^{2/3}}{me}}\xi$ is the non-local parameter that is often defined as a function of the Fermi velocity, v_F by

$$\beta^2 = \frac{2}{3}\frac{E_F}{m_e} = \frac{v_F^2}{3}. \tag{4.14}$$

E_F being the Fermi energy $\frac{h^2(3\pi^2 n_0)^{2/3}}{2m_e}$. This expression is very close to the most likely value of β as suggested by the Duke's experiments[11].

Maxwell's equations are thus coupled to equation (4.13). In the harmonic regime this equation becomes

$$\beta^2\vec{\nabla}(\vec{\nabla}.\vec{P}) + (\omega^2 + i\gamma\omega)\vec{P} = -\varepsilon_0\omega_p^2\vec{E}. \tag{4.15}$$

Because of the term $\beta^2\vec{\nabla}(\vec{\nabla}.\vec{P})$ the effective polarization is not local any more - the electric field in one location has an impact on the polarization further away. The pressure term that is responsible for the apparition of the spatial dispersion can be linked to the repulsion between electrons - and exchange interaction can totally be integrated into this term, because, just like Coulomb forces, it leads to repulsion between electrons[11].

4.2 Non-Locality

Now we will shortly see how Maxwell's equations can be solved in the framework of the hydrodynamic model for multilayers. Using Maxwell's equations, the polarization $\vec{P}_f$ corresponding solely to the free electrons that obey the hydrodynamic equations can be easily written

$$\vec{P}_f = \frac{\epsilon_0.\omega_p^2}{\omega^2 + i\gamma\omega}\left(\vec{E} - (1+\chi_b)\frac{\beta^2}{\omega_p^2}\nabla\left(\nabla.\vec{E}\right)\right). \tag{4.16}$$

In a metallic layer, two kinds of waves can actually be distinguished. First the transverse wave, characterized by $\vec{\nabla}.\vec{E} = 0$ then waves for which $\vec{\nabla} \wedge \vec{E} = \vec{0}$ and consequently $\vec{H} = \vec{0}$. Such waves are of course said to be longitudinal and they correspond to the equivalent of sound in the plasma.

If $\nabla.\vec{E} = 0$, $\vec{\nabla}.\vec{P}_f = \vec{0}$ then everything reduces to the standard Maxwell's equations with a Drude model.

$$\partial_z E_x - \partial_x E_z = i\omega\,\mu_0\,H_y \tag{4.17}$$

$$E_x = \frac{1}{i\omega\varepsilon_0\,\varepsilon_m}\partial_z H_y \tag{4.18}$$

$$E_z = -\frac{1}{i\omega\varepsilon_0\,\varepsilon_m}\partial_x H_y. \tag{4.19}$$

so that, inside the metal, the fields can be written (in layer j)

$$H_y = (A_j e^{-\kappa_t z} + B_j e^{\kappa_t z})e^{i(k_x x-\omega t)} \tag{4.20}$$

$$E_x = \frac{i\kappa_t}{\omega\varepsilon_0\varepsilon_m}(A_j e^{-\kappa_t z} - B_j e^{\kappa_t z})e^{i(k_x x-\omega t)} \tag{4.21}$$

$$E_z = \frac{-k_x}{\omega\varepsilon_0\varepsilon_m}(A_j e^{-\kappa_t z} + B_j e^{\kappa_t z})e^{i(k_x x-\omega t)}, \tag{4.22}$$

where $\kappa_t = \sqrt{k_x^2 - \varepsilon_m\,k_0^2}$.

For the longitudinal wave, which is curl free, we can write that

$$\partial_z E_x = \partial_x E_z. \tag{4.23}$$

and finally

$$E_x^\ell = \frac{1}{\omega\varepsilon_0}(C_j e^{-\kappa_\ell z} + D_j e^{\kappa_\ell z})\big]e^{i(k_x x-\omega t)} \tag{4.24}$$

$$E_z^\ell = \frac{-\kappa_\ell}{ik_x\omega\varepsilon_0}(C_j e^{-\kappa_\ell z} - D_j e^{\kappa_\ell z})e^{i(k_x x-\omega t)} \tag{4.25}$$

with a wavevector

$$\kappa_\ell = \sqrt{k_x^2 + \frac{\omega_p^2}{\beta^2}\left(\frac{1}{\chi_f} + \frac{1}{1+\chi_b}\right)} \tag{4.26}$$

which is given by the dispersion relation of bulk plasmons. Here ω_p is the plasma frequency of the considered metal, and χ_f and χ_b are the susceptibilities associated with the free and bound electrons, respectively ($\epsilon_m = 1 + \chi_b + \chi_f$).

Because it is possible to write analytically the form of the fields inside a metallic layer, it is possible to come up with a scattering matrix method that is particularly well suited for non-locality[6]. This method will not be described here, but it has been implemented in Moosh, making it particularly easy to simulate the optical response of a metallo-dielectric multilayer. I have used this to study the sensitivity of a gap-plasmon prism coupler to spatial dispersion.

4.3 Gap-Plasmon Resonance and non-locality

The idea that such a structure has a chance to be more sensitive to non-locality comes from the dispersion relation for the gap-plasmon in the framework of the hydrodynamic model. It presents a simple form[28]

$$\frac{\kappa_z}{\epsilon_d}\tanh\frac{\kappa_z\, h}{2}+\frac{\kappa_t}{\epsilon}=\Omega \tag{4.27}$$

where $\Omega=\frac{k_x^2}{\kappa_l}\left(\frac{1}{\epsilon}-\frac{1}{1+\chi_b}\right)$ which differs from the local one solely because of Ω. When $\beta=0$, in the local case, $\Omega=0$, but otherwise it is not null and thus perturbates the wavevector of the gap-plasmon when it becomes large (since Ω is proportional to k_x^2).

While the surface plasmon never reaches large wavevectors because of the losses that produce a bend-back close enough to ω_{sp}, the gap-plasmon can reach high effective indexes when the gap decreases. Our prediction was then that it should be easier to witness an impact of non-locality on a gap-plasmon prism coupler than on a surface plasmon prism coupler. The only way however to reach quite high effective indexes and to still be able to couple to the gap-plasmon is to use a high index prism coupler. Here we have thus considered TiO_2. The configuration is reminded on figure 4.1.

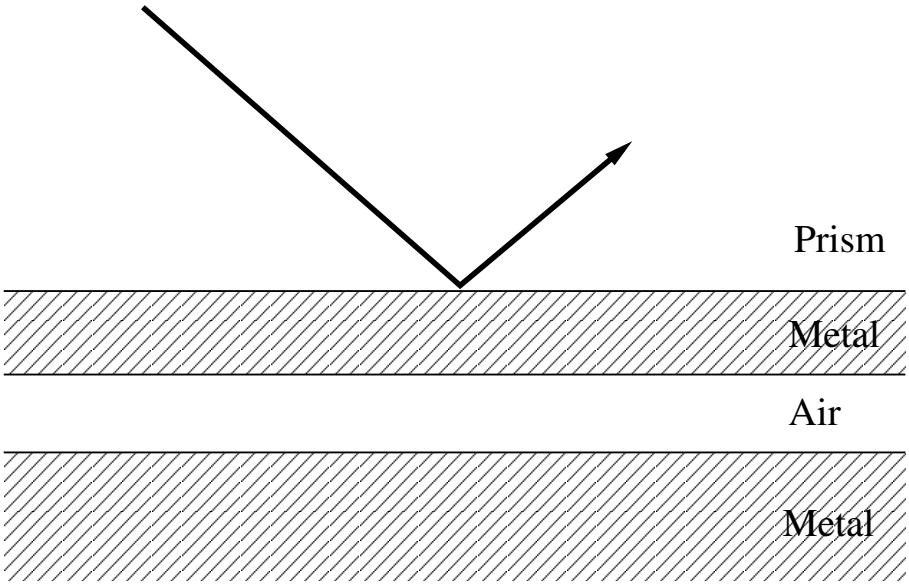


FIGURE 4.1: A gap-plasmon prism coupler, with a high index prism on top, a metallic layer through which the gap-plasmon is coupled and a metallic substrate.

We have thus used Moosh to study the impact of various geometrical parameters on this configuration. There are two crucial parameters: the thickness of the layer attached to the prism, and the width of the gap, which controls the effective index. In addition, a working wavelength has to be chosen. Since we are considering a gap-plasmon here, there is no need to be

close to ω_{sp} to reach high effective indexes. For larger wavelength, more in the visible, or almost infrared part of the spectrum, the bound electrons play a smaller role and do not absorb as much as in the blue part of the spectrum. We have thus chosen $\lambda = 650nm$.

For the gold attached to the prism, we have tried different thicknesses, while keeping the gap constant. This has convinced us that, while using thicker gold layer could improve the slowing down of the gap-plasmon, it was more important to keep it quite thin (18 nm) to be able to couple the gap-plasmon efficiently. We underline that 18 nm is much thinner than what is usually considered for surface plasmon couplers. Figure 4.2 shows the impact of this first layer on the reflection coefficient of the structure, when the gap-plasmon is excited through the prism.

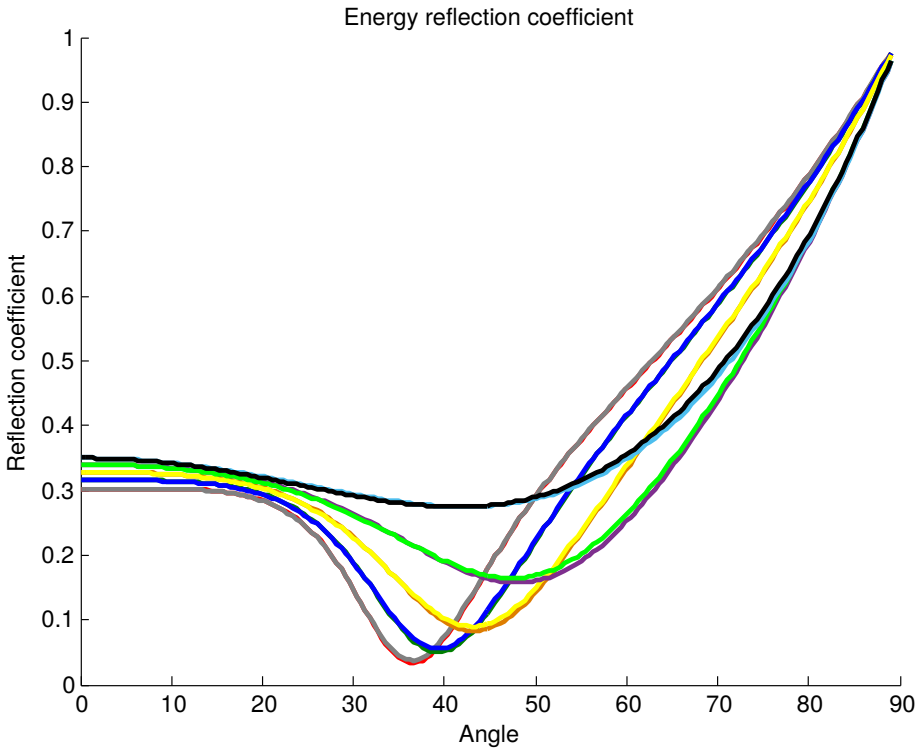


FIGURE 4.2: A wavelength $\lambda = 500$nm the same thickness of the gold layer(20nm) and varying the thickness of the second medium, the red and gray curves (Non-local,local respectively) with a thickness of the additional layer 50 nm, the green and blue curves (Non-local,local respectively) with a thickness of the additional layer 40 nm, the orange and yellow curves (Non-local,local respectively) with a thickness of the additional layer 30 nm, the purple and light green (Non-local,local respectively) with a thickness of the additional layer 20 nm, and the light blue and black curves (Non-local,local respectively) with a thickness of the additional layer 10 nm.

Finally, after having settled for 18 nm for the gold intermediate layer, we have tried to see if even for relatively small effective indexes, the impact of spatial dispersion could be seen. The results are shown on figure 4.3 for

various width of the gap. Our first conclusion is clearly that the narrower the gap, the larger the effective index, and thus the larger the impact of non-locality. When the gap, however, becomes too narrow, the effective index of the gap-plasmon is so high that is larger than the index of the prism, and the guided mode cannot be coupled any more.

The main result here is that a shift of 1 to 2° can be observed between the local and the nonlocal simulations, indicating a clear impact of nonlocality. While this impact may seem modest, at least it is measurable - it is within reach of current experimental setups.

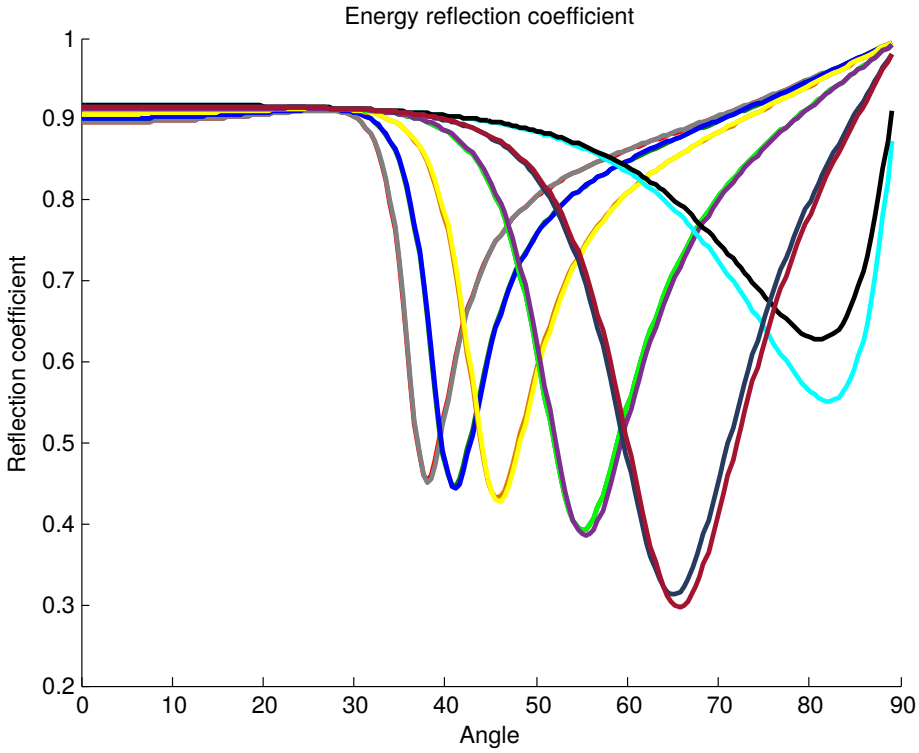


FIGURE 4.3: A wavelength $\lambda = 700$nm the same thickness of the gold layer (20nm) and varying the thickness of the second medium, the red and gray curves (Non-local,local respectively) with a thickness of the second layer is 50 nm, the green and blue curves (Non-local,local respectively) with a thickness of the gold layer 40 nm, the orange and yellow curves (Non-local,local respectively) with a thickness of the gold layer 30 nm, the purple and light green (Non-local,local respectively) with a thickness of the gold layer 20 nm, and the light blue and black curves (Non-local,local respectively) with a thickness of the gold layer 10 nm.

4.4 Conclusion

In this chapter, I have detailed the hydrodynamic model and explained how it is possible to solve analytically Maxwell's equations, coupled to the equation that links the external electric field and the effective polarization corresponding to the free electron currents inside the metal. Using a scattering matrix method that has been implemented in Moosh, I was able to study the influence of spatial dispersion on a gap-plasmon prism coupler, showing that a small but measurable shift could be measurable in such a configuration. We hope this will pave the way for future experiments.

Conclusion

The main contribution of this work is undoubtedly the generalization of Yariv and Yeh's theorem, which shows that any guided mode in a plasmonic multilayer has a group velocity that is equal to its energy velocity. Such a a conclusion could seem trivial, but in the process, we have learned a few important points. The energy velocity we are dealing with is simply the energy that is conveyed by the electromagnetic field alone and it does not include the energy conveyed by the free electrons in the metal. In order to get a physical insight into why exactly the group velocity is so low, there is thus no need to consider the contribution of free electrons. Moreover, the energy density that appears in our calculations has the exact form of the electromagnetic energy density that is used for dispersive media by Brillouin, Landau or Loudon[32]. This means that our derivation constitutes a fourth, original, way to justify the form chosen for the energy density.

Importantly, the theorem we have demonstrated shows that in order to obtain an analytical expression for the group velocity, it is as simple to calculate the flux of the Poynting vector and the mean energy density and do the ratio. Doing so presents an advantage: the Poynting balance allows to understand the plasmonic slowdown. This is the low group velocity and high effective index experienced by guided mode is certain conditions: for surface plasmons and gap-plasmons near the surface plasmon frequency, and for gap-plasmon either close to this peculiar frequency, or at any frequency when the gap closes. Such a regime can be seen as a consequence of the plasmonic drag: the fact that the Poynting vector inside a metal is opposite to the Poynting inside a dielectric for a mode that is guided in a plasmonic waveguide. The mean flux of the Poynting vector, divided but the mean energy density perpendicularly to the mode propagation gives the energy velocity and thus the group velocity. When we close the gap between two metals, the gap-plasmon propagating in between propagates more and more in the metal, and is thus more subject to this plasmonic drag. Its energy velocity and thus its group velocity decrease strongly, and finally, since the group velocity is the derivative of ω with respect to the propagation constant, this means that the propagation constant can only strongly increase. Yariv and Yeh's theorem, for plasmonics, thus present a real interest which is not obvious for dielectric-only waveguides.

Using Moosh[12], an open source library that I have helped to develop through a lot of testing, I have tried in this manuscript to illustrate many different situations in nanophotonics and plasmonics. I hope this will help illustrate its potential both for research and teaching. For teaching because a nice image can be extremely informative. In research a seemingly simple tool as Moosh, can be use to reveal very fundamental phenomena, like the

influence of the repulsion between free electrons in metal on the optical response of a metallic structure. I have, in the last chapter of this manuscript, studied a surprizingly simple structure where these effects can clearly be seen, and that could be perhaps realized one day. This structure belongs to a new class of plasmonic resonating architectures (supporting gap-plasmon resonances), that are all more likely to be sensitive to these phenomena and the spatial dispersion they provoke.

Bibliography

[1] F. Abelès. "Recherche sur la propagation des ondes électromagnétiques sinusoïdales dans les milieux stratifiés : Application aux couches minces". In: *Ann. Phys. (Paris)* 5 (1950), p. 596.

[2] Gleb M. Akselrod et al. "Probing the mechanisms of large Purcell enhancement in plasmonic nanoantennas". In: *Nature Photonics* 8 (2014), pp. 835–840.

[3] Harry A Atwater. "The promise of plasmonics". In: *Scientific American* 296.4 (2007), pp. 56–62.

[4] William L Barnes, Alain Dereux, and Thomas W Ebbesen. "Surface plasmon subwavelength optics". In: *Nature* 424.6950 (2003), pp. 824–830.

[5] Jessica Benedicto et al. "Large negative lateral shifts due to negative refraction". In: *Optics letters* 36.13 (2011), pp. 2539–2541.

[6] Jessica Benedicto et al. "Numerical tool to take nonlocal effects into account in metallo-dielectric multilayers". In: *JOSA A* 32.8 (2015), pp. 1581–1588.

[7] Sergey I Bozhevolnyi and Thomas Søndergaard. "General properties of slow-plasmon resonant nanostructures: nano-antennas and resonators". In: *Optics express* 15.17 (2007), pp. 10869–10877.

[8] Léon Brillouin. *Wave propagation and group velocity*. Vol. 8. Academic Press, 2013.

[9] Andrea Cattoni et al. "$\lambda 3/1000$ plasmonic nanocavities for biosensing fabricated by soft UV nanoimprint lithography". In: *Nano letters* 11.9 (2011), pp. 3557–3563.

[10] GV Chester and A Thellung. "The law of Wiedemann and Franz". In: *Proceedings of the Physical Society* 77.5 (1961), p. 1005.

[11] C Ciracì et al. "Probing the ultimate limits of plasmonic enhancement". In: *Science* 337.6098 (2012), pp. 1072–1074.

[12] Josselin Defrance et al. "Moosh: A Numerical Swiss Army Knife for the Optics of Multilayers in Octave/Matlab". In: *Journal of Open Research Software* 4.1 (2016).

[13] P Drude. "On the electron theory of metals". In: *Ann Phys* 1 (1900), pp. 566–613.

[14] P Drude, CR Mann, and RA Millikan. "The theory of optics (1902)". In: *New York etc.: Longmans, Green, and Co* 1 (2008).

[15] Paul Drude. "Zur elektronentheorie der metalle". In: *Annalen der Physik* 306.3 (1900), pp. 566–613.

[16] S. Enoch and N. Bonod. "Plasmonics". In: *Springer Series in Optical Sciences 167* 1.1 (2012), pp. 1–20.

[17] G. Granet and B. Guizal. "Efficient implementation of the coupled-wave method for metallic lamellar gratings in TM polarization". In: *J. Opt. Soc. Am. A* 13 (1996), p. 1019.

[18] Peter Kaspar et al. "Average light velocities in periodic media". In: *J. Opt. Soc. Am. B* 30.11 (2013), pp. 2849–2854. DOI: 10.1364/JOSAB.30.002849. URL: http://josab.osa.org/abstract.cfm?URI=josab-30-11-2849.

[19] E Kretschmann. "Decay of non radiative surface plasmons into light on rough silver films. Comparison of experimental and theoretical results". In: *Optics Communications* 6.2 (1972), pp. 185–187.

[20] Erwin Kretschmann and Heinz Raether. "Notizen: radiative decay of non radiative surface plasmons excited by light". In: *Zeitschrift für Naturforschung A* 23.12 (1968), pp. 2135–2136.

[21] Joseph R Lakowicz et al. "Plasmon-controlled fluorescence: A new detection technology". In: *Biomedical Optics 2006*. International Society for Optics and Photonics. 2006, pp. 609909–609909.

[22] P. Lalanne and G. M. Morris. "Highly improved convergence of the coupled-wave method for TM polarization". In: *J. Opt. Soc. Am. A* 13 (1996), p. 779.

[23] Gaëtan Lévêque, Olivier JF Martin, et al. "Optical interactions in a plasmonic particle coupled to a metallic film". In: *Opt. Express* 14.21 (2006), pp. 9971–9981.

[24] Christopher Loo et al. "Immunotargeted nanoshells for integrated cancer imaging and therapy". In: *Nano letters* 5.4 (2005), pp. 709–711.

[25] Alexei A Maradudin, J Roy Sambles, and William L Barnes. *Modern Plasmonics*. Vol. 4. Elsevier, 2014.

[26] J. C. Maxwell. "On physical lines of forces". In: *The London, Edinburgh and Dublin Philosophical Magazine and Journal of Science* 4 (1861), p. 161.

[27] J Clerk Maxwell. "A dynamical theory of the electromagnetic field". In: *Philosophical transactions of the Royal Society of London* 155 (1865), pp. 459–512.

[28] Antoine Moreau, Cristian Ciraci, and David R Smith. "Impact of nonlocal response on metallodielectric multilayers and optical patch antennas". In: *Physical Review B* 87.4 (2013), p. 045401.

[29] Antoine Moreau et al. "Controlled-reflectance surfaces with film-coupled colloidal nanoantennas". In: *Nature* 492.7427 (2012), pp. 86–89.

[30] Lukas Novonty and Bert Hecht. "Principles of Nano-optics". In: *Cambridge University Press* 1.1 (2006), pp. 378–380. URL: www.cambridge.org/9780521832243.

[31] Lukas Novotny and Bert Hecht. *Principles of nano-optics*. Cambridge university press, 2012.

[32] Frederico Dias Nunes et al. "Electromagnetic energy density in dispersive and dissipative media". In: *JOSA B* 28.6 (2011), pp. 1544–1552.

[33] D Patrick O'Neal et al. "Photo-thermal tumor ablation in mice using near infrared-absorbing nanoparticles". In: *Cancer letters* 209.2 (2004), pp. 171–176.

[34] Andreas Otto. "Excitation of nonradiative surface plasma waves in silver by the method of frustrated total reflection". In: *Zeitschrift für Physik* 216.4 (1968), pp. 398–410.

[35] John Brian Pendry. "Negative refraction makes a perfect lens". In: *Physical review letters* 85.18 (2000), p. 3966.

[36] S Pillai et al. "Surface plasmon enhanced silicon solar cells". In: *Journal of applied physics* 101.9 (2007), p. 093105.

[37] Alexander Poddubny et al. "Hyperbolic metamaterials". In: *Nature Photonics* 7.12 (2013), pp. 948–957.

[38] Alexander W Powell et al. "Plasmonic Gas Sensing Using Nanocube Patch Antennas". In: *Advanced Optical Materials* (2016).

[39] Aleksandar D Rakić et al. "Optical properties of metallic films for vertical-cavity optoelectronic devices". In: *Applied optics* 37.22 (1998), pp. 5271–5283.

[40] M Scalora et al. "Transparent, metallo-dielectric, one-dimensional, photonic band-gap structures". In: *Journal of Applied Physics* 83.5 (1998), pp. 2377–2383.

[41] Richard A Shelby, David R Smith, and Seldon Schultz. "Experimental verification of a negative index of refraction". In: *Science* 292.5514 (2001), pp. 77–79.

[42] DR Smith and D Schurig. "Electromagnetic wave propagation in media with indefinite permittivity and permeability tensors". In: *Physical Review Letters* 90.7 (2003), p. 077405.

[43] Viktor G Veselago. "The electrodynamics of substances with simultaneously negative values of and?" In: *Soviet physics uspekhi* 10.4 (1968), p. 509.

[44] Ting Xu et al. "All-angle negative refraction and active flat lensing of ultraviolet light". In: *Nature* 497.7450 (2013), pp. 470–474.

[45] Amnon Yariv and Pochi Yeh. "Electromagnetic propagation in periodic stratified media. II. Birefringence, phase matching, and x-ray lasers". In: *JOSA* 67.4 (1977), pp. 438–447.

[46] Pochi Yeh. *Optical waves in layered media*. Vol. 61. Wiley-Interscience, 2005.